THE ASTROPHYSICAL JOURNAL SUPPLEMENT SERIES, 98:1–32, 1995 May

THE FIRST CALTECH–JODRELL BANK VLBI SURVEY. I. λ = 18 CENTIMETER OBSERVATIONS OF 87 SOURCES

A. G. POLATIDIS AND P. N. WILKINSON
University of Manchester, Nuffield Radio Astronomy Laboratories, Jodrell Bank, Macclesfield, Cheshire SK11 9DL, UK
AND
W. XU, A. C. S. READHEAD, T. J. PEARSON, G. B. TAYLOR, AND R. C. VERMEULEN
Owens Valley Radio Observatory, California Institute of Technology 105-24, Pasadena, CA 91125
Received 1993 December 30; accepted 1994 November 2

ABSTRACT

We present the first results from the first Caltech–Jodrell Bank VLBI survey (the CJ1 survey). The CJ1 sample includes 135 radio sources with total flux density 1.3 Jy > $S_{6\,cm} \geq 0.7$ Jy, declination $\delta_{1950} \geq 35°$, and Galactic latitude $|b^{II}| > 10°$. It extends the flux density limit of the complete "PR" sample studied by Pearson & Readhead from 1.3 to 0.7 Jy and increases the total number of sources from 65 to 200.

The complete survey includes VLBI images at both λ-18 and 6 cm of all the objects in the extended sample that have cores strong enough to be mapped with the Mark II VLBI system. These images provide a large enough sample to study, for example, the variety of morphologies exhibited by compact radio sources, cosmological evolution, superluminal motion, and misalignment between parsec-scale and kiloparsec-scale radio structures.

In this paper we present λ-18 cm VLBI observations of 56 CJ1 and 31 PR sources made in 1990–1991, including images of 82 sources. The observations were made with a "snapshot" technique in which each source was observed in three 20–30-minute scans using an array of 12–16 antennas. The images have resolution 3–10 mas and dynamic range greater than 100:1. Later papers in the series will present the remaining λ-18 cm observations, the λ-6 cm observations, and the analysis and interpretation of the results.

Subject headings: quasars: general — radio continuum: galaxies — surveys — techniques: interferometric

1. PARSEC-SCALE OBSERVATIONS OF COMPACT RADIO SOURCES

VLBI observations have revealed a variety of radio structures in active galactic nuclei (AGNs) ranging from asymmetric core–jets to compact symmetric objects (CSOs) (e.g., Readhead, Pearson, & Unwin 1984; Conway et al. 1994; Wilkinson et al. 1994) and the complex structures observed in some compact steep-spectrum sources (CSS) (e.g., Fanti et al. 1990a). It is not yet known whether these morphological differences reflect fundamental differences in the central engines or environmental differences in the parent galaxies. To clarify the relationships between the various types of source and to elucidate the underlying causes of the different radio structures one can study either a few representative sources in detail or well-defined samples of sources to investigate their statistical properties.

So far, largely due to the limited observing time devoted to VLBI, the first approach has dominated VLBI efforts. However, several groups have observed complete, albeit small, samples of AGNs. The largest complete sample to date has been the "PR" sample (Pearson & Readhead 1981, 1988 [PR88]). This sample contains 65 objects, selected from the MPIfR-NRAO S4 and S5 surveys (Pauliny-Toth et al. 1978; Kühr et al. 1981) of which 45 have been imaged with VLBI. The S4 and S5 surveys were made at a short wavelength (λ-6 cm) and hence the selection favors objects where the dominant radio emission arises in a compact, flat-spectrum component. PR88 proposed a classification scheme for all 65 sources in the sample based on the milliarcsecond-scale morphology of the sources, their large-scale radio structure and their radio spectra. There are five major classes of radio-loud AGNs, some of which are divided into subclasses.

Other significant surveys have also been made. For example a sample of 13 flat-spectrum sources, selected from the S5 survey with $\delta > 70°$ and $S_{6\,cm} > 1$ Jy, has been studied by astronomers from MPIfR (Eckart et al. 1987; Witzel et al. 1988). The weak cores of lobe-dominated sources have been studied by several sets of workers; thus far results on more than 30 objects have been published (e.g., Zensus & Porcas 1987; Hooimeyer et al. 1992; Giovannini et al. 1992; Hough, Vermeulen, & Readhead 1993). Samples of ~50 compact steep-spectrum sources selected from the 3CR and the Peacock & Wall (1982) catalogs have been observed at multiple wavelengths by an international group of astronomers (e.g., Fanti et al. 1985, 1990b; Sanghera 1992; Dallacasa et al. 1994). A group mainly from Brandeis University has been investigating the milliarcsecond-scale polarization of quasars and BL Lac objects; observations of 24 objects have been published so far (e.g., Cawthorne et al. 1993a,b). Finally Wehrle et al. (1992) have been studying a sample of 41 sources with flux density that has exceeded 4.5 Jy at λ-3.8 cm at any epoch.

These studies, and follow-up work on individual objects, have begun to delineate the different morphological classes of compact objects in AGNs and their distinctive properties, have demonstrated that the phenomenon of superluminal motion is common in most of these classes, and have focused attention on a number of particularly interesting objects. However it is

clear that a larger complete sample of sources is required to tackle a variety of interesting astronomical questions, many of which arose from these smaller surveys.

2. THE FIRST CALTECH-JODRELL BANK VLBI SURVEY (CJ1)

The large number of apparently different classes of AGNs, as revealed by the PR88 analysis, first raises the question of whether the full range of morphologies has been observed and identified. In addition the size of the PR sample is too small for many interesting statistical studies to be performed; in particular some classes contain only one or two members and statistical tests *within* these classes are impossible. We therefore decided to expand PR's work by making observations of a significantly larger, complete flux-density–limited sample of radio sources. The program is a collaboration between the California Institute of Technology (Caltech) and N.R.A.L. Jodrell Bank (University of Manchester). Since it is the first such survey we identify it as the first Caltech–Jodrell Bank or CJ1 survey.[1]

Our principal astronomical aims are (1) To test the PR classification scheme and to add to it any new types of objects we might observe. (2) To provide a sample large enough to make interesting statistical studies both as a whole and within and between different classes. In particular, we can investigate the distribution of misalignments between the milliarcsecond scale and the arcsecond scale (PR88) and study the cosmological evolution of different classes using the luminosity-volume test. The relation between VLBI angular size and redshift can also be used as a probe of universal geometry (Kellermann 1993; Gurvits 1993). Testing the applicability of "Unified Schemes" is another goal of this study. (3) To provide first-epoch observations of a large sample of candidate sources for superluminal motion studies (Vermeulen & Cohen 1994). (4) To look for possible small-separation gravitational lens systems.

In order to have a large enough sample of sources for statistical studies, we decided to select a set of sources which, when combined with the PR sample, would treble the total number of objects available for study. We therefore selected sources from the S4 and S5 surveys by lowering the flux density limit used by PR, but otherwise following PR's two remaining selection criteria. Our sample thus obeys the following selection criteria: (1) flux density at 6 cm: 1.3 Jy $> S_{6\ \mathrm{cm}} \geq$ 0.7 Jy; (2) declination (B1950.0) $\delta \geq 35°$; and (3) Galactic latitude $|b^{\mathrm{II}}| > 10°$. The selection was based on the flux densities measured at the epoch of the S4 and S5 surveys, and since many of the sources are variable a selection made from measurements at another epoch would result in a slightly different sample.

There are 137 objects in the S4 and S5 surveys which conform to the above criteria. Of them one, 1758+666, is identified with a planetary nebula and another, 1038+528, consists of two independent quasars (Owen, Wills, & Wills 1980), neither of which is strong enough to satisfy, on its own, the flux density selection criterion. These two sources have been excluded and thus our final *CJ1 sample* contains 135 objects. Together with the PR sample we therefore have a total of 200 objects for statistical studies.

Complementary observing programs have been undertaken to obtain arcsecond scale radio maps of CJ1 sources for which an adequate map was not available in the literature and to complete the optical identifications and measure redshifts. Redshifts for 26 objects were reported by Xu et al. (1994); further results will be reported in later papers in this series.

The PR survey was made at λ-6 cm but for the CJ1 survey we decided to make VLBI observations both at λ-6 cm and λ-18 cm in order to take advantage of the complementary resolution and surface brightness sensitivity provided at these two wavelengths. Maps at two wavelengths were expected to clarify ambiguous cases and hence to increase the reliability of the classification.

In order to complete the dual-wavelength observations of such a large sample within a practical time span, we used a "snapshot" observing technique, which will be explained in detail below. The observations were made using the NRAO Mark II recording system, principally because of the availability of the JPL/Caltech Block II correlator which can process data from 16 telescopes simultaneously.

The sensitivity of the narrowband (1.8 MHz) Mark II system limits the number of sources that can be imaged to those with a compact component stronger than ~100 mJy. For reasons of time economy, we did not perform a "finding" survey like PR; instead, we collated from the literature arcsecond and subarcsecond resolution maps, mainly made with the VLA and MERLIN, for all the sources in the sample. We also collected radio spectral information for all the sources, mainly from Kühr et al. (1979). Using the radio structure and radio spectral information we sorted the sources into the following categories:

1. Sources which were almost certain to have structure that can be mapped with the Mark II system. These include sources with overall angular size less than 2″ and all objects observed with VLBI by Preston et al. (1985) for which at least 20% of the total flux density is detected on intercontinental baselines.
2. Sources which had been previously observed with VLBI and for which the maps were of sufficient quality to allow us to classify the source unambiguously.
3. Sources which do not contain strong enough compact components to be mapped by Mark II VLBI. These sources are predominantly large, lobe-dominated sources with weak or nondetected core.

Table 1 lists the 135 sources in the CJ1 sample. Of these, there are 81 sources in category 1 that we have observed at λ-18 cm. Furthermore, to complete the information on the PR sample, we decided to observe the 28 objects from the PR sample that had not been observed previously with VLBI at λ-18 cm. We also included the previously mapped objects 0538+498, 1458+518, and 1807+698 as a check on the snapshot technique (see Appendix A). The 31 PR sources observed are listed in Table 2.

The observations took place in nine observing sessions, four at λ-18 cm and five at λ-6 cm wavelength, and were completed within two and a half years starting in 1990 March. In this paper we discuss the observations and the data analysis for 87 sources observed in three of the four λ-18 cm observing ses-

[1] The second Caltech–Jodrell Bank or CJ2 survey of 193 flat- and peaked-spectrum sources is reported by Taylor et al. (1994) and Henstock et al. (1995).

TABLE 1

THE COMPLETE CJ1 SAMPLE

Source (1)	Other (2)	R.A. (3)	Declination (4)	S_{11cm} (5)	S_{6cm} (6)	$S_{2.8cm}$ (7)	ID (8)	V (9)	z (10)	Ref (11)	λ18 cm VLBI (12)
0010+405 ...	4C40.01	00 13 31.131	40 51 37.15	1.18	1.05	0.78	G	17.9	0.255	2	1990 Sep
0010+775 ...	...	00 13 11.7	77 48 47	1.32	0.781	0.48	G	18.0	0.326	1	1991 Nov
0013+790 ...	3C6.1	00 16 32.3	79 16 52	2.01	1.044	0.46	G	22.0	0.840	3	...
0022+390 ...	OA 026	00 25 26.157	39 19 35.45	0.78	0.859	0.91	Q	19.8	1.946	1	1991 Sep
0048+509 ...	3C22.0	00 50 56.2	51 12 04	1.28	0.760	0.33	G	22.0	0.937	2	...
0102+480 ...	...	01 05 49.930	48 19 03.18	1.09	0.982	0.75	EF	...	...	2	1991 Jun
0106+729 ...	3C33.1	01 09 44.3	73 11 57	1.86	0.890	...	G	19.5	0.181	4	...
0206+355 ...	4C35.03	02 09 38.6	35 47 51	1.43	0.894	0.58	G	13.0	0.0373	2	...
0218+357 ...	OD 330	02 21 05.470	35 56 13.72	1.03	1.17	0.90	BL	20.0	>0.685	2,5	1991 Nov
0220+397 ...	3C65.0	02 23 42.8	40 00 52	1.59	0.770	0.31	G	23.0	1.176	2	...
0248+430 ...	...	02 51 34.537	43 15 15.83	0.96	1.21	1.20	Q	18.6	1.316	2	1991 Jun
0258+350 ...	4C34.09	03 01 42.37	35 12 20.7	1.31	0.926	0.65	G	13.5	0.0165	2	...
0307+444 ...	4C44.07	03 10 31.2	44 35 48	0.98	0.733	...	Q	18.8	1.165	2	...
0309+390 ...	4C39.11	03 12 26.7	39 16 30	1.12	0.728	0.34	G	18.2	0.161	2	...
0402+379 ...	4C37.11	04 05 49.263	38 03 32.24	1.47	1.15	0.69	G	18.5	0.055	1	1990 Sep
0407+747 ...	4C74.08	04 13 17.0	74 51 07	1.67	0.962	0.49	G	19.1	–	1	...
0602+673 ...	...	06 07 52.672	67 20 55.42	0.83	1.07	1.08	Q	20.6	...	2	1990 Sep
0615+820 ...	...	06 26 03.007	82 02 25.57	1.02	0.999	0.86	Q	17.5	0.710	3	10
0620+389 ...	...	06 24 19.022	38 56 48.72	0.89	0.874	...	Q	20.0	3.470	1	1991 Nov
0642+449 ...	OH 471	06 46 32.026	44 51 16.59	1.27	0.778	0.90	Q	18.5	3.406	2	1991 Nov
0646+600 ...	OH 577.1	06 50 31.256	60 01 44.55	0.69	0.788	0.46	Q	18.9	0.455	2	1991 Sep
0650+371 ...	...	06 53 58.283	37 05 40.61	0.77	0.971	0.71	Q	18.2	1.982	2	1991 Sep
0651+542 ...	3C171.0	06 55 14.9	54 09 00	1.99	1.16	0.53	G	18.9	0.2384	2	...
0702+749 ...	3C173.1	07 09 18.4	74 49 32	1.46	0.789	0.32	G	18.9	0.292	4	...
0703+426 ...	4C42.23	07 06 41.9	42 31 58	1.67	0.985	0.60	G	15.0	0.060	2	...
0707+476 ...	...	07 10 46.105	47 32 11.14	1.29	0.998	1.37	Q	18.2	1.292	2	1991 Sep
0707+689 ...	4C68.08	07 13 14.1	68 52 09	1.13	0.749	0.42	Q	20.5	1.141	1	11
0716+714 ...	...	07 21 53.449	71 20 36.36	0.97	1.121	2.00	BL	13.2	–	1	1991 Nov
0734+805 ...	3C184.1	07 43 01.4	80 26 26	1.92	1.134	0.27	G	17.0	0.118	3	...
0740+828 ...	...	07 50 57.764	82 41 58.03	1.29	0.931	0.65	Q	18.5	1.991	1	1991 Jun
0746+483 ...	OI 478	07 50 20.438	48 14 53.56	0.70	0.796	0.79	Q	18.4	1.951	2	1991 Nov
0755+379 ...	3C189	07 58 28.8	37 47 12	1.79	1.26	0.86	G	14.9	0.0433	2	1991 Jun
0805+410 ...	...	08 08 56.652	40 52 44.88	0.94	0.766	1.08	Q	19.0	1.420	1	1991 Nov
0812+367 ...	OJ 320	08 15 25.945	36 35 15.14	1.03	1.01	0.98	Q	18.0	1.025	2	1990 Sep
0816+526 ...	4C52.18	08 19 47.7	52 32 26	1.22	0.776	0.42	G	18.0	0.189	2	...
0818+472 ...	3C197.1	08 21 33.6	47 02 37	1.16	0.860	0.30	G	16.5	0.1301	2	...
0820+560 ...	OJ 535	08 24 47.237	55 52 42.67	1.08	0.917	0.88	Q	18.0	1.417	2	1991 Sep
0821+394 ...	4C39.23	08 24 55.484	39 16 41.90	1.10	0.993	1.18	Q	18.5	1.216	2	1991 Sep
0827+378 ...	4C37.24	08 31 10.0	37 42 10	1.37	0.930	0.57	Q	18.1	0.914	2	(1991 Sep)
0828+493 ...	OJ 448	08 32 23.217	49 13 21.04	1.17	1.02	0.96	BL	18.8	0.548	2	1991 Jun
0833+585 ...	...	08 37 22.410	58 25 01.84	0.50	1.11	1.23	Q	18.0	2.101	2	1991 Jun
0844+540 ...	4C54.17	08 47 53.9	53 52 35	1.07	0.732	0.43	G	15.0	0.0453	2	...
0900+428 ...	4C42.28	09 04 15.628	42 38 04.77	0.97	0.761	0.72	G	19.9	...	2	1991 Nov
0917+449 ...	...	09 20 58.459	44 41 53.98	0.54	0.803	1.01	Q	19.0	2.18	2	1991 Nov
0917+624 ...	OK 630	09 21 36.231	62 15 52.18	0.87	0.996	1.36	Q	19.5	1.446	2	1991 Sep
0936+361 ...	3C223.0	09 39 52.7	35 53 58	2.06	1.29	0.72	G	17.1	0.1368	2	...
0938+399 ...	3C223.1	09 41 24.0	39 44 42	1.23	0.870	0.49	G	16.4	0.1075	2	...
0945+664 ...	4C66.09	09 49 12.165	66 14 59.59	1.62	1.22	0.77	G	21.6	...	2	(1991 Jun)
0955+476 ...	OK 492	09 58 19.670	47 25 07.83	0.71	0.739	0.75	Q	18.0	1.873	2	1991 Nov
1003+830 ...	...	10 10 15.774	82 50 14.38	0.78	0.716	0.66	G	20.5	0.322	1	1991 Sep
1007+416 ...	4C41.21	10 10 27.6	41 32 38	1.04	0.706	0.50	Q	16.5	0.611	2	...
1015+359 ...	OL 326	10 18 10.988	35 42 39.44	0.63	0.916	1.04	Q	18.5	1.226	2	1991 Sep
1020+400 ...	4C40.25	10 23 11.566	39 48 15.38	1.06	0.866	1.18	Q	17.5	1.254	1	1991 Nov
1030+415 ...	...	10 33 03.708	41 16 06.23	1.02	1.13	1.48	Q	18.2	1.120	2	1991 Jun
1030+585 ...	3C244.1	10 33 33.7	58 14 43	1.95	1.12	0.51	G	19.0	0.428	2	...

TABLE 1—*Continued*

Source (1)	Other (2)	R.A. (3)	Declination (4)	S_{11cm} (5)	S_{6cm} (6)	$S_{2.8cm}$ (7)	ID (8)	V (9)	z (10)	Ref (11)	λ18 cm VLBI (12)
1039+811 ...	...	10 44 23.063	80 54 39.44	0.90	1.144	0.78	Q	16.5	1.254	3	10
1044+719 ...	...	10 48 27.620	71 43 35.93	0.74	0.707	0.96	Q	19	1.15	6	1991 Sep
1053+704 ...	...	10 56 53.619	70 11 45.90	0.65	0.710	0.96	Q	18.5	2.492	1	1991 Sep
1053+815 ...	...	10 58 11.539	81 14 32.67	0.96	0.770	1.20	G	18.5	0.706	1	1991 Sep
1056+432 ...	3C247	10 58 58.8	43 01 24	1.55	0.949	0.40	G	21.5	0.7489	2	...
1058+726 ...	4C72.16	11 01 48.807	72 25 37.11	1.07	0.778	0.56	Q	17.4	1.45	7	1991 Sep
1100+772 ...	3C249.1	11 04 13.9	76 58 58	1.33	0.772	0.45	Q	15.7	0.311	4	...
1101+384 ...	Mkr 421	11 04 27.315	38 12 31.79	0.77	0.725	0.79	BL	13.1	0.0308	2	1991 Nov
1111+408 ...	3C254	11 14 38.7	40 37 20	1.45	0.790	0.32	Q	18.0	0.734	2	...
1128+385 ...	OM 346.9	11 30 53.282	38 15 18.55	0.89	0.771	0.93	Q	16.0	1.733	1	1991 Nov
1137+660 ...	3C263.0	11 39 57.1	65 47 49	1.73	1.04	0.57	Q	16.3	0.649	2	...
1138+594 ...	4C59.16	11 40 48.9	59 12 31	1.23	0.767	0.43	EF	...	...	2	(1991 Nov*)
1144+402 ...	...	11 46 58.298	39 58 34.30	1.05	0.941	1.55	Q	18.5	1.088	1	1991 Sep
1144+542 ...	...	11 46 44.204	53 56 43.09	0.71	0.878	0.73	Q	20.5	2.201	1	1991 Nov
1150+497 ...	4C49.22	11 53 24.466	49 31 08.83	1.56	1.11	1.48	Q	17.1	0.334	2	1991 Nov
1150+812 ...	...	11 53 12.499	80 58 29.15	1.25	1.181	1.10	Q	18.5	1.250	3	10
1152+551 ...	4C55.22	11 55 28.2	54 53 34	1.33	0.843	0.52	G	16.0	0.050	2	...
1203+645 ...	3C268.3	12 06 24.7	64 13 37	2.00	1.16	0.51	G	20.0	0.371	2	12
1213+350 ...	4C35.28	12 15 55.602	34 48 15.21	1.21	1.01	0.79	Q	20.1	0.851	2	1991 Jun
1213+538 ...	4C53.24	12 15 29.6	53 35 58	1.40	0.904	0.37	Q	18.0	1.065	2	...
1216+487 ...	ON 428	12 19 06.415	48 29 56.17	0.96	1.08	1.05	Q	18.5	1.076	2	1991 Jun
1225+368 ...	ON 343	12 27 58.726	36 35 11.82	1.58	0.767	0.26	Q	21.5	1.974	1	13
1242+410 ...	ON470.5	12 44 49.188	40 48 06.14	1.16	0.744	0.53	Q	19.0	0.813	1	1991 Nov
1250+568 ...	3C277.1	12 52 26.3	56 34 20	1.53	1.05	0.41	Q	17.9	0.321	2	14
1311+678 ...	4C67.22	13 13 27.3	67 36 05	1.45	0.923	0.50	EF	...	...	2	1991 Sep
1317+520 ...	4C52.27	13 19 46.196	51 48 05.76	0.92	0.716	0.45	Q	17.0	1.060	2	1991 Nov
1319+428 ...	3C285	13 21 17.8	42 35 14	1.23	0.760	0.48	G	16.0	0.0794	2	...
1333+459 ...	...	13 35 21.960	45 42 38.25	0.57	0.757	0.66	Q	18.5	2.449	1	1991 Nov
1333+589 ...	4C58.26	13 35 25.928	58 44 00.29	0.72	0.826	0.74	EF	...	...	2	1991 Sep
1336+391 ...	3C288	13 38 49.9	38 51 09	1.76	0.992	0.37	G	16.5	0.2459	2	...
1342+663 ...	...	13 44 08.679	66 06 11.65	0.61	0.817	0.89	Q	19.4	1.351	1	1991 Sep
1347+539 ...	4C53.28	13 49 34.657	53 41 17.04	1.00	0.962	0.91	Q	17.3	0.978	1	1991 Jun
1349+647 ...	3C292	13 50 42.0	64 29 35	1.06	0.720	0.75	G	20.7	0.713	2	...
1357+769 ...	...	13 57 55.370	76 43 21.05	0.58	0.844	0.60	SO	19.0	...	8	1991 Sep
1418+546 ...	OQ 530	14 19 46.598	54 23 14.79	0.94	1.09	1.43	BL	15.5	0.152	2	1990 Sep
1419+419 ...	3C299	14 21 05.6	41 44 49	1.61	0.900	0.39	G	18.4	0.367	2	...
1435+638 ...	...	14 36 45.803	63 36 37.87	1.41	1.24	1.01	Q	15.0	2.068	2	1990 Sep
1437+624 ...	OQ 663	14 38 44.8	62 11 55	1.39	0.862	0.44	Q	19.0	1.090	2	1991 Sep
1438+385 ...	OQ 363	14 40 22.337	38 20 13.63	0.88	0.770	0.56	Q	21.6	...	2	1991 Nov
1441+522 ...	3C303	14 43 02.7	52 01 38	1.55	0.940	0.81	G	17.0	0.141	2	...
1448+634 ...	3C305	14 49 21.5	63 16 14	1.60	0.920	0.47	G	13.7	0.041	2	...
1504+377 ...	OR 306	15 06 09.530	37 30 51.13	0.97	1.10	1.56	G	21.2	0.674	2	1990 Sep
1547+507 ...	OR 580	15 49 17.468	50 38 05.79	0.69	0.738	0.65	Q	18.5	2.169	2	1991 Sep
1549+628 ...	3C325	15 49 58.4	62 41 22	1.84	0.830	0.42	G	21.0	0.86	2	...
1557+708 ...	4C70.19	15 57 31.0	70 41 25	1.76	1.02	...	G	14.0	0.026	1	...
1627+444 ...	3C337	16 28 53.1	44 19 14	1.57	0.910	0.50	G	21.0	0.635	2	...
1637+626 ...	3C343.1	16 38 28.2	62 34 44	2.23	1.20	0.50	G	20.7	0.750	2	12
1637+826 ...	NGC6251	16 32 31.971	82 32 16.38	1.37	0.978	0.73	G	14.3	0.0243	3	15
1638+398 ...	NRAO512	16 40 29.633	39 46 46.03	1.08	1.16	1.72	Q	16.5	1.666	2	1990 Sep
1656+477 ...	...	16 58 02.779	47 37 49.24	0.73	0.923	0.86	Q	18.2	1.622	2	1991 Sep
1656+482 ...	4C48.41	16 57 46.879	48 08 33.05	0.89	0.776	0.81	EF	...	...	2	1991 Sep
1658+471 ...	3C349.0	16 59 29.5	47 02 44	1.88	1.14	0.58	G	19.0	0.205	2	...
1704+608 ...	3C351.0	17 04 41.3	60 44 30	2.03	1.21	0.59	Q	15.3	0.371	2	...
1719+357 ...	OT 332	17 21 09.491	35 42 16.07	0.64	0.859	0.84	Q	17.5	0.263	2	1991 Nov
1732+389 ...	OT 355	17 34 20.579	38 57 51.45	0.67	1.15	0.89	Q	19.0	0.976	2	1991 Jun

TABLE 1—*Continued*

Source (1)	Other (2)	R.A. (3)	Declination (4)	S_{11cm} (5)	S_{6cm} (6)	$S_{2.8cm}$ (7)	ID (8)	V (9)	z (10)	Ref (11)	λ18 cm VLBI (12)
1734+508 ...	...	17 35 49.005	50 49 11.57	0.60	0.803	0.72	EF	...	...	2	1991 Sep
1738+476 ...	OT 465	17 39 57.130	47 37 58.37	0.84	0.904	0.85	BL	19.5	0.316	1	1991 Jun
1751+441 ...	OT 486.4	17 53 22.650	44 09 45.67	0.59	1.04	1.22	Q	19.5	0.871	2	1990 Sep
1758+388 ...	OT 398	18 00 24.765	38 48 30.70	0.42	0.916	1.62	Q	17.8	2.092	2	1991 Jun
1800+440 ...	OU 401	18 01 32.315	44 04 21.90	0.63	1.02	1.12	Q	16.8	0.663	2	1990 Sep
1819+396 ...	4C39.56	18 21 20.9	39 42 45	1.78	0.971	0.38	G	19.0	...	2	16
1825+743 ...	3C379.1	18 24 33.0	74 20 57	1.05	0.728	0.35	G	18.0	0.256	4	...
1832+474 ...	3C381	18 33 46.2	47 27 21	2.30	1.29	0.79	G	17.2	0.1605	2	...
1833+653 ...	3C383	18 33 43.6	65 21 38	1.23	0.799	0.38	G	17.0	0.161	2	...
1842+681 ...	...	18 42 33.642	68 09 25.23	0.87	0.810	1.50	Q	17.9	0.473	1	1991 Jun
1843+356 ...	OU 373	18 45 35.110	35 41 16.72	0.95	0.812	0.49	G	21.9	...	2	1991 Nov
1926+611 ...	...	19 27 30.443	61 17 32.88	–	0.721	0.80	BL	17.5	–	1	1991 Jun
1940+504 ...	3C402	19 41 46.0	50 35 45	1.72	0.933	–	G	14.0	0.0239	2	...
1943+546 ...	OV 573	19 44 31.514	54 48 07.07	1.20	0.850	0.50	G	17.7	0.263	2	1991 Jun
2007+777 ...	...	20 05 30.999	77 52 43.25	0.82	1.279	1.10	BL	16.5	0.342	9	10
2010+723 ...	4C72.28	20 09 52.302	72 29 19.35	1.08	0.917	0.75	BL	19.0	–	1	(1991 Jun*)
2104+763 ...	3C427.1	21 04 07.5	76 33 07	1.93	0.997	0.37	G	21.1	0.572	3	...
2207+374 ...	4C37.65	22 09 21.424	37 42 18.23	1.23	0.791	0.48	Q	18.5	1.493	1	1991 Sep
2214+350 ...	OY 324	22 16 20.011	35 18 14.18	0.74	0.824	0.56	Q	18.0	0.510	2	1991 Jun
2229+695 ...	...	22 30 36.468	69 46 28.07	0.62	0.812	0.80	G	19.6	–	1	1991 Jun
2253+417 ...	OY 489	22 55 36.708	42 02 52.54	1.17	0.990	1.00	Q	18.8	1.476	2	1991 Jun
2255+416 ...	4C41.45	22 57 22.072	41 54 16.52	1.42	0.993	0.62	Q	20.9	1.724	1	1991 Jun
2311+469 ...	4C46.47	23 13 48.1	47 12 16	1.11	0.726	0.43	Q	17.9	0.742	1	(1991 Jun*)
2323+435 ...	OZ 438	23 25 42.3	43 46 58	1.35	1.01	0.58	G	18.0	0.145	2	17
2324+405 ...	3C462	23 26 55.9	40 48 09	1.51	1.12	0.57	G	19.9	0.394	2	(1990 Sep)

NOTES.—Table 1 is published in computer-readable form in the AAS CD-ROM Series, Vol. 4.

Col. (1): Source name according to IAU convention. Col. (2): Alternative source name. Cols. (3)–(4): J2000.0 right ascension and declination. Positions specified with a precision of 0.″01 are from the Jodrell Bank–VLA Astrometric Survey (Patnaik et al. 1992, Tables 2 and 4; and unpublished observations); the remaining positions have been compiled from a variety of publications via the NASA Extragalactic Database (NED). Cols. (5)–(7): Total flux density (Jy) at λ-11, 6, and 2.8 cm (Pauliny-Toth et al. 1978; Kühr et al. 1981). Col. (8): Optical identification: BL, BL Lac object; EF, empty field; G, galaxy; Q, quasar; SO, stellar object. Col. (9): Visual magnitude. Col. (10): Redshift; "–" indicates a featureless spectrum. Col. (11): Reference for optical identification, magnitude, and redshift. Col. (12): Date of λ-18 cm VLBI observation or reference to published observation. Parentheses indicate that the source was observed but was not mapped; in three cases (marked with an asterisk) this is because the a priori position assumed for correlations was wrong, while in the other cases the source was too heavily resolved. An ellipsis indicates that the source was not observed because it does not contain a compact component strong enough for detection with Mark-II VLBI.

REFERENCES.—(1) Xu et al. 1994; (2) Stickel & Kühr 1994; (3) Stickel, Meisenheimer, & Kühr 1994; (4) Spinrad et al. 1985; (5) Browne et al. 1993; (6) Henstock, Browne, & Wilkinson 1995; (7) Jackson 1989; (8) Palomar Observatory Sky Survey; (9) Hewitt & Burbidge 1993; (10) Eckart et al. 1987; (11) Sanghera 1992; (12) Fanti et al. 1985; (13) Dallacasa et al. 1994; (14) Foulsham 1989; (15) Jones et al. 1986; (16) Dallacasa et al. 1990; (17) Sanghera 1989; (18) Lawrence et al. 1995.

sions. The observations of the 25 sources in the remaining λ-18 cm session are discussed in the accompanying Paper II (Thakkar et al. 1995). The λ-6 cm results will be presented in Paper III (Xu et al. 1995).

3. OBSERVATIONS

3.1. *Snapshot Method*

The images obtained in the PR survey have a typical resolution of 1–2 mas and a dynamic range (defined as the ratio of the peak brightness to the rms noise in an area of blank sky) between 50:1 and 300:1. To achieve our astronomical goals the CJ1 images at the two wavelengths had to be of comparable or better quality. However a project as large as the CJ1 survey would be impractical with the long track observations used by PR. It would require ~1600 hr of observing time and, given the limited amount of time available to VLBI networks, would take at least 8 years to complete. In view of the large number of telescopes that now regularly take part in VLBI observations we decided instead to use a "snapshot" observing scheme.

We carried out a series of tests and simulations to determine the optimum combination of scans required to achieve our observational goals with an array of 12–16 telescopes (see our Appendix; Polatidis 1993). We found that with three 20 minute scans, sources of rather greater complexity than those in PR's maps could reliably be mapped with a dynamic range greater than 100:1. Although a larger number of shorter scans would provide more uniform u, v coverage, and hence even better images, the loss of data each time the telescopes slew from source to source would decrease the number of data points severely. Because of this reduction in observing efficiency our actual observations were made with scans of 30 minutes each. This provided us with at least 20 minutes of data for most scans, and at least a few minutes of data even from scans where a telescope has to unwind completely in azimuth.

TABLE 2

SOURCES FROM THE PR SAMPLE OBSERVED AT λ = 18 CENTIMETERS

Source (1)	Other (2)	R.A. (3)	Declination (4)	S_{11cm} (5)	S_{6cm} (6)	$S_{2.8cm}$ (7)	ID (8)	V (9)	z (10)	Ref (11)	λ18 cm VLBI (12)
0108+388 ...	OC 314	01 11 37.319	39 06 28.09	1.00	1.35	0.86	G	22	0.6703	18	1990 Sep
0133+476 ...	OC 457	01 36 58.595	47 51 29.10	2.19	3.26	...	Q	19	0.859	18	1990 Sep
0404+768 ...	4C 76.03	04 10 45.0	76 56 47	4.00	2.79	1.80	G	22	0.5985	18	1990 Sep
0538+498 ...	3C 147	05 42 36.1	49 51 07	13.0	8.18	4.14	Q	17.8	0.545	18	1990 Sep
0711+356 ...	OI 318	07 14 24.818	35 34 39.79	1.83	1.51	0.97	Q	17	1.620	18	1991 Jun
0723+679 ...	3C 179	07 28 10.9	67 48 48	1.58	1.31	0.98	Q	18.0	0.8436	18	1990 Sep
0804+499 ...	OJ 508	08 08 39.667	49 50 36.53	1.53	2.07	1.62	Q	17.5	1.4321	18	1990 Sep
0814+425 ...	OJ 427	08 18 16.000	42 22 45.41	2.21	1.68	2.47	BL	17.7	0.2453	18	1990 Sep
0831+557 ...	4C 55.16	08 34 54.903	55 34 21.09	7.45	5.60	2.82	G	17.5	0.2404	18	1990 Sep
0850+581 ...	4C 58.17	08 54 41.996	57 57 29.92	0.87	1.41	1.55	Q	18	1.322	18	1991 Jun
0859+470 ...	4C 47.29	09 03 03.990	46 51 04.14	1.87	1.78	1.47	Q	18.7	1.462	18	1990 Sep
0906+430 ...	3C 216	09 09 33.5	42 53 46	2.39	1.78	1.41	Q	18.5	0.670	18	1990 Sep
0923+392 ...	4C 39.25	09 27 03.014	39 02 20.85	4.82	8.90	12.2	Q	17.9	0.699	18	1991 Jun
0945+408 ...	4C 40.24	09 48 55.339	40 39 14.58	1.26	1.39	1.29	Q	17.5	1.252	18	1991 Jun
1458+718 ...	3C 309.1	14 59 07.6	71 40 20	5.04	3.34	1.96	Q	16.8	0.9021	18	1990 Sep
1624+416 ...	4C 41.32	16 25 57.670	41 34 40.63	1.58	1.31	1.14	Q	22	2.550	18	1990 Sep
1633+382 ...	4C 38.41	16 35 15.493	38 08 04.50	2.50	4.08	6.03	Q	18	1.807	18	1990 Sep
1637+574 ...	OS 562	16 38 13.457	57 20 23.98	0.98	1.44	1.73	Q	17	0.7487	18	1990 Sep
1642+690 ...	4C 69.21	16 42 07.849	68 56 39.76	1.42	1.43	1.90	Q	19.2	0.751	18	1990 Sep
1652+398 ...	4C 39.49	16 53 52.217	39 45 36.61	1.44	1.42	1.19	G	13.8	0.0328	18	1990 Sep
1739+522 ...	4C 51.37	17 40 36.978	52 11 43.40	1.93	1.99	1.37	Q	18.5	1.381	18	1990 Sep
1749+701 ...	...	17 48 32.841	70 05 50.77	1.89	1.09	1.39	BL	17.0	0.7699	18	1991 Nov
1807+698 ...	3C 371	18 06 50.681	69 49 28.11	2.21	2.33	1.81	G	14.2	0.050	18	1990 Sep
1823+568 ...	4C 56.27	18 24 07.069	56 51 01.49	1.51	1.67	2.28	BL	18.4	0.6634	18	1990 Sep
1845+797 ...	3C 390.3	18 42 08.9	79 46 18	6.61	4.32	2.02	G	15	0.0569	18	1990 Sep
1954+513 ...	OV 591	19 55 42.739	51 31 48.55	1.57	1.43	1.33	Q	18.5	1.2230	18	1990 Sep
2021+614 ...	OW 637	20 22 06.682	61 36 58.81	2.17	2.31	1.95	G	19.5	0.228	18	1990 Sep
2200+420 ...	BL Lac	22 02 43.292	42 16 39.98	5.15	4.75	5.82	BL	14.5	0.0688	18	1990 Sep
2342+821 ...	...	23 44 03.7	82 26 40	2.30	1.30	0.65	Q	20.5	0.7344	18	1990 Sep
2351+456 ...	4C 45.51	23 54 21.678	45 53 04.24	1.48	1.41	1.04	Q	20.6	1.9864	18	1990 Sep
2352+495 ...	OZ 488	23 55 09.459	49 50 08.34	2.18	1.77	1.12	G	19.7	0.2383	18	1990 Sep

NOTES.—Table 2 is published in computer-readable form in the AAS CD-ROM Series, Vol. 4.

Col. (1): Source name according to IAU convention. Col. (2): Alternative source name. Cols. (3)–(4): J2000.0 right ascension and declination. Positions specified with a precision of 0.01 are from the Jodrell Bank–VLA Astrometric Survey (Patnaik et al. 1992, Tables 2 and 4; and unpublished observations); the remaining positions have been compiled from a variety of publications via the NASA Extragalactic Database (NED). Cols. (5)–(7): Total flux density (Jy) and λ-11, 6, at 2.8 cm (Pauliny-Toth et al. 1978; Kühr et al. 1981). Col. (8): Optical identification: BL, BL Lac object; G, galaxy; Q, quasar; SO, stellar object. Col. (9): Visual magnitude. Col. (10): Redshift. Col. (11): Reference for optical identification, magnitude, and redshift. Col. (12): Date of λ-18 cm VLBI observation.

REFERENCE.—(18) Lawrence et al. 1995.

To maximize the u, v coverage we tried to schedule three scans as widely spaced as possible within the mutual visibility "window" during which the source could be seen by all the antennas. For some low-declination sources ($\delta \approx 35°$–$37°$) the mutual visibility window was quite short ($\approx$4 hr) and the resulting u, v coverage contains significant gaps, although the image quality is still adequate for our purposes (see Fig. 1). The source changes were optimized to provide the shortest slewing time between sources in order to avoid significant data loss from some of the slower telescopes. The equatorially mounted telescopes in the array, WSRT and Green Bank, posed additional constraints in scheduling. In the case of WSRT, where the hour angle coverage is limited to ±6 hr from the meridian, we inevitably scheduled a few scans when the source could not be observed, but this did not affect the image quality significantly.

3.2. λ-18 Centimeter Observations

The λ-18 cm VLBI observations for the CJ1 survey were completed in four observing sessions. Here we present the observations of 87 sources taken in 1990 September, in 1991 June, and in 1991 November; the observations of the remaining 25 objects taken in 1991 September are presented in Paper II (Thakkar et al. 1995). All available telescopes of the European (EVN) and the US (USVN) VLBI networks, including the partly completed VLBA (Napier et al. 1994), were scheduled to participate.[2] In addition, telescopes in the Soviet Union participated in some of the observations.

The data were recorded using the NRAO Mark II system with an effective bandwidth of 1.8 MHz centered at 1.665 GHz. Left circular polarization (LCP) (IEEE convention) was recorded. All telescopes of the EVN and the USVN were

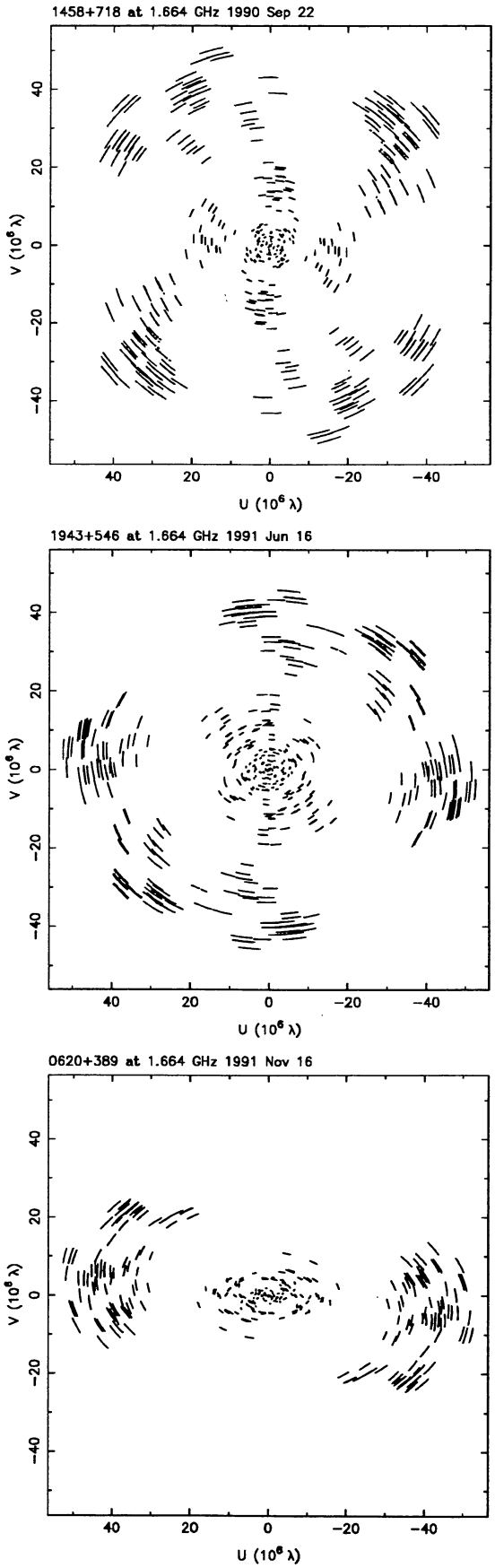

equipped with hydrogen masers as frequency and timing standards, and rubidium atomic clocks were used at the telescopes of the Soviet Union.

In 1990 September, 13 telescopes were scheduled to observe 37 sources in a 60 hr observing session. Useful data were obtained from 12 telescopes for most of the observing session. In 1991 June, 17 telescopes took part in the 42 hr observations of 27 sources. In 1991 November, 13 telescopes participated successfully and 23 sources were observed in a 41 hour session. The participating telescopes and their characteristics are listed in Table 3. Examples of the u, v coverage obtained are shown in Figure 1.

3.3. *Correlation and Fringe Fitting*

The data were correlated with the JPL/Caltech Block II correlator which enabled us to process nearly all the observations in a single correlation pass. The output of the correlator is an estimate of complex fringe visibility sampled at intervals of 2 s on each baseline, at four frequencies within the 2 MHz band, with the phase referenced to an *a priori* model of the source position, antenna locations, and atmosphere. Before the data can be averaged over the full bandwidth and longer time-intervals, the residual phase gradients in time and frequency due to delay and rate errors in the *a priori* model must be estimated and removed. This is the process of "fringe fitting." Fringe fitting was performed using the NRAO Astronomical Image Processing System (AIPS) task FRING, an implementation of the Schwab & Cotton (1983) algorithm. A solution interval of 5 minutes—comparable with the coherence time—and a point-source model were used. The "reference telescope" was chosen to be Effelsberg whenever possible, otherwise the Green Bank telescope was used. After correction of the delays and rates found by FRING, the visibilities were coherently averaged across the observing band, and then the phases were self-calibrated using a point-source model with a solution interval of 10 s, using the program DIFMAP in the Caltech VLBI package (Pearson 1991; Shepherd, Pearson, & Taylor 1994). In the 1991 June observing session, the coherence time was much shorter than in the other sessions, apparently as a result of ionospheric scintillation. For this session it was found that a shorter self-calibration interval of 2 s improved the signal-to-noise ratio for sources with more than 350 mJy in a compact component.

For the three sources 1138+594, 2010+723, and 2311+469, we were unable to find fringes on all baselines. This was due to large errors ($\geq 10''$) in the *a priori* source positions used for the correlator model. We were thus unable to map these three sources. Three other sources, 0010+775, 0945+664, and 2324+405, were heavily resolved and were detected only on

[2] The VLBA, the VLA, and the 140 foot (43 m) Green Bank telescope are instruments of the National Radio Astronomy Observatory, which is operated by Associated Universities, Inc., under cooperative agreement with the National Science Foundation.

FIG. 1.—Examples of the sampling of the projected-baseline (u, v) plane obtained in the snapshot observations at declinations 71°, 54°, and 38°.

TABLE 3

TELESCOPE CHARACTERISTICS

Telescope	Code	Location	Diam (m)	1990 Sep	1991 Jun	1991 Nov	T_{sys} (K)	T_{sys} (Jy)	Sensitivity (K/Jy)
Onsala	S	Sweden	25		√		32	348	0.093
Effelsberg	B	Germany	100	√	√	√	54[a]	36	1.5[a]
WSRT	W	Netherlands	5×25			√	58	125	0.46
Lovell	J	Jodrell Bank, UK	76	√	√	√	38	44	0.86
Medicina	L	Bologna, Italy	32	√	√	√	53	530	0.1
Simeiz	R	Crimea, USSR	22	√	√	√	104	1155	0.09
Evpatoria	Ev	Crimea, USSR	70		√		100	143	0.7
Pushchino	Pu	Moscow, USSR	22		√		450	5000	0.09
Bear Lake	Bl	Moscow, USSR	64		√		89	118	0.75
NRAO	G	Green Bank, WV, USA	43	√	√	√	21	70	0.3
Haystack	K	Westford, MA, USA	36	√	√		96	1116	0.086
VLBA_PT	PT	Pie Town, NM, USA	25	√	√	√	31	321	0.097
VLBA_KP	KP	Kitt Peak, AZ, USA	25	√	√	√	33	334	0.099
VLBA_LA	LA	Los Alamos, NM, USA	25	√	√	√	31	295	0.104
VLBA_NL	NL	North Liberty, IA, USA	25		√	√	32	366	0.088
VLA[b]	Y	Socorro, NM, USA	25	√	√	√	34	378	0.089
OVRO	O	Owens Valley, CA, USA	40	√	√	√	53	254	0.21

[a] Estimate only; actual performance quoted in janskys.

[b] the VLA was used in single antenna mode.

Cols. (1)–(3): The name, the code used and the location of each telescope. Affiliations: S: Onsala Space Observatory; B: Max-Planck-Institüt für Radioastronomie; W: Westerbork Synthesis Radio Telescope, NFRA; J Nuffield Radio Astronomy Laboratories; L: Istituto di Radioastronomia; R, Ev, Bl, Pu: IKI Moscow; G: National Radio Astronomy Observatory; K: Haystack Observatory; PT, KP,LA, FD, NL: National Radio Astronomy Observatory VLBA; Y: National Radio Astronomy Observatory VLA; O: Owens Valley Radio Observatory. Col. (4): The diameter of each telescope (in meters). Cols. (5)–(7): A tick indicates whether the telescope participated in that session. Cols. (8)–(10): The system temperature in kelvins and in janskys and the sensitivity in kelvins per jansky of each telescope. The values quoted are representative of the three sessions.

short baselines (less than ~500 km). We were able to make a low-resolution map of 0010+775 but were not able to make useful maps of the other two sources.

After fringe fitting and phase self-calibration the visibility data were first averaged coherently across the observing band and then averaged in time intervals of 60 s. The uncertainties of the averaged data were estimated from the scatter of the points within the averaging interval.

3.4. *Amplitude Calibration*

Calibration of the data was performed using the method described by Cohen et al. (1975). The calibration of the correlation coefficients was based on the peak telescope sensitivity and a normalized gain-elevation curve for each telescope. At λ-18 cm telescope gains are very weakly dependent on elevation so flat gain curves were adequate for most of the telescopes. The system temperature values supplied by each observatory were inspected and any obviously erroneous values, probably due to radio interference, were deleted. The Caltech program CAL was used to apply the amplitude calibration to the raw visibilities.

In practice the *a priori* amplitude calibration is rarely much better than ~5% and is often 10% in error, hence it is necessary to observe calibrator sources with known structures (but only slightly resolved) which are strong enough to be detected with high signal-to-noise ratio on all baselines. For our observations we used the sources 0552+398 and 1739+522 as calibrators. The observations of the calibrators were spread out over the entire time span of each session to monitor changing conditions in the array. Although neither calibrator is unresolved at λ-18 cm, their visibilities can be fitted by single Gaussians. The calibration source data were self-calibrated with the program DIFMAP using the Gaussian models; the gain of each telescope was allowed to vary by a single multiplicative factor for the complete run on the calibrator. DIFMAP produced a set of correction factors to be applied on a telescope-by-telescope basis in CAL.

FIG. 2.—The λ = 18 cm VLBI maps of 82 sources. For each source the top panel shows the naturally weighted, higher resolution map, and the bottom panel the tapered map. Logarithmic contour levels are used in all maps, drawn at $-2, -1, 1, 2, 4, 8, 16, \cdots 1024 \times 3\ \sigma$ (where σ is the rms noise measured in an empty region of the map). The FWHM contour of the elliptical Gaussian restoring beam is shown hatched in the lower left-hand corner. The peak flux density, rms noise, and parameters of the restoring beam are given in Table 4. The angular scale is marked in milliarcseconds and, where the source redshift is known, the linear scale of each map is indicated in the lower right-hand corner (assuming $H_0 = 100$ km s^{-1} Mpc^{-1} and $q_0 = 0.5$). Note that the field of view of the tapered map is usually larger than that of the uniformly weighted map. For 0010 + 775, which was heavily resolved, we present only a low-resolution map. FITS images corresponding to the maps presented in Fig. 2 are published in the AAS CD-ROM Series, Vol. 4.

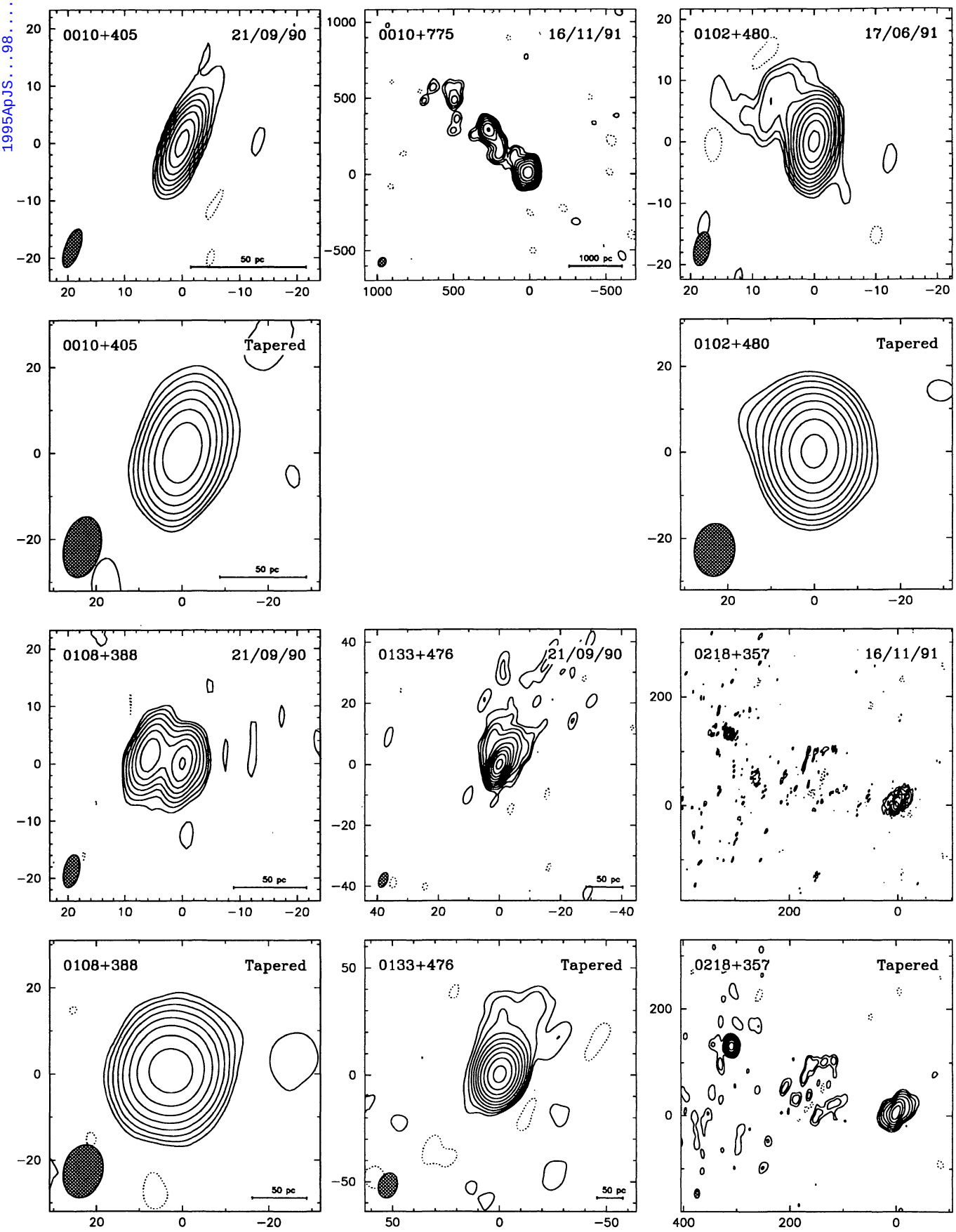

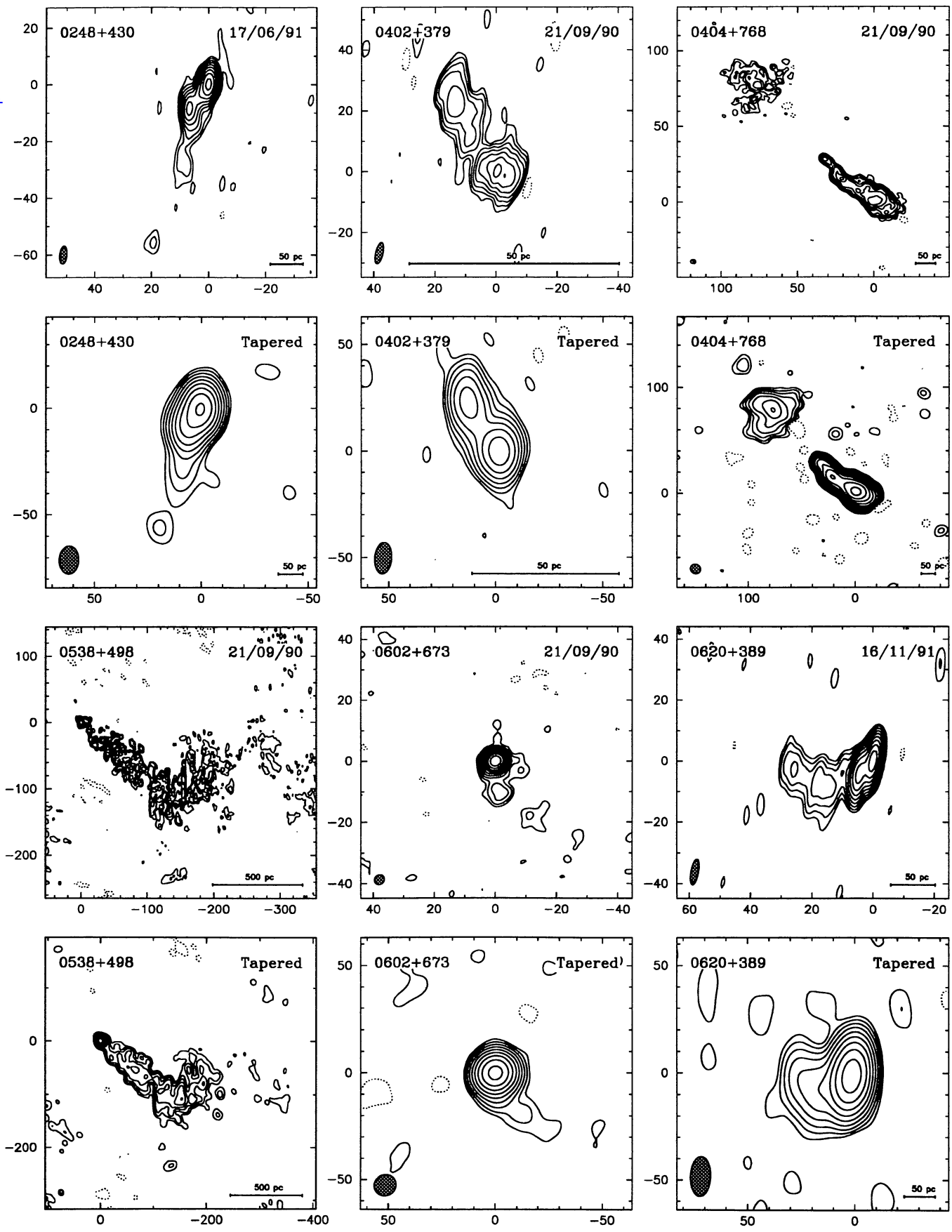

FIG. 2.—*Continued*

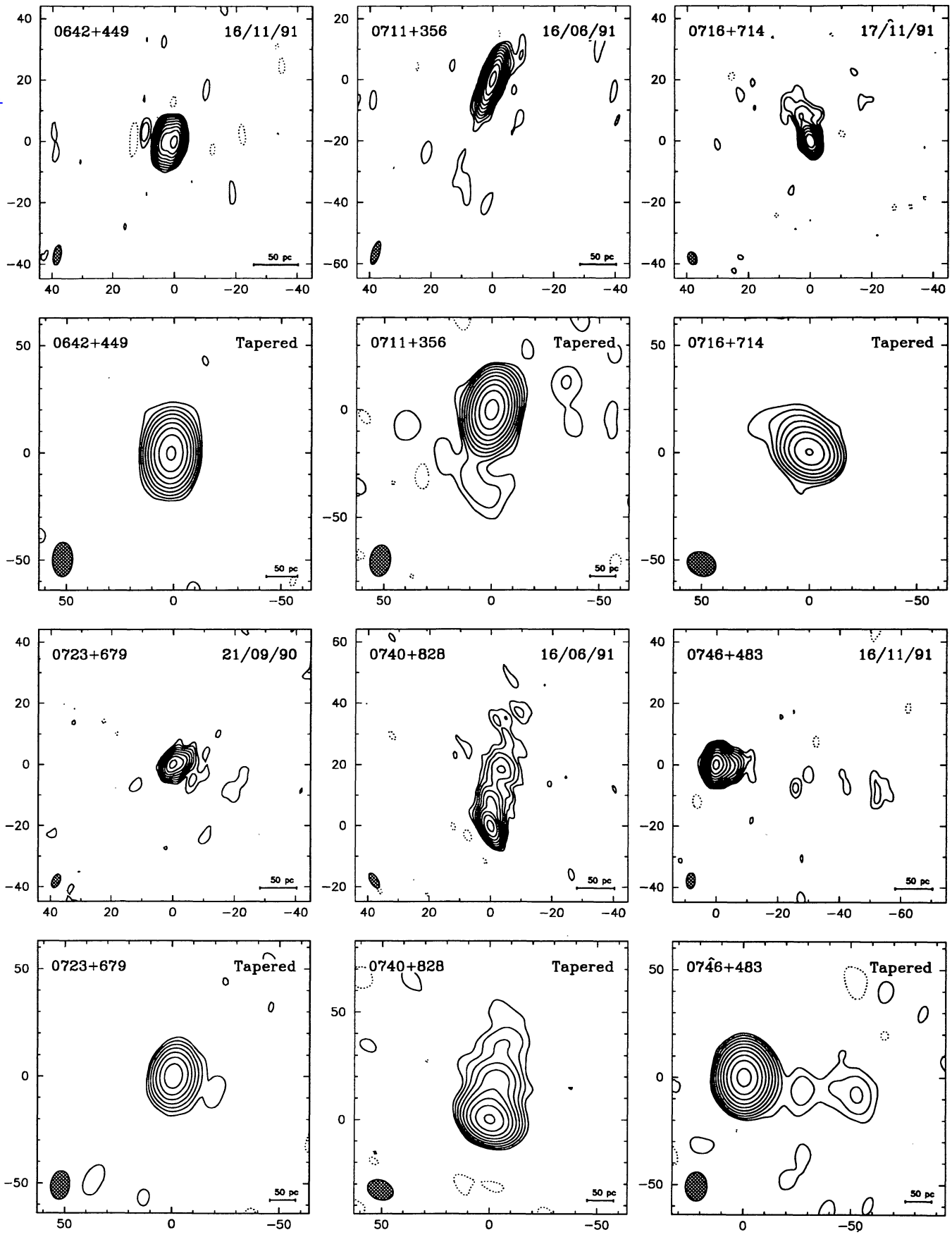

FIG. 2.—*Continued*

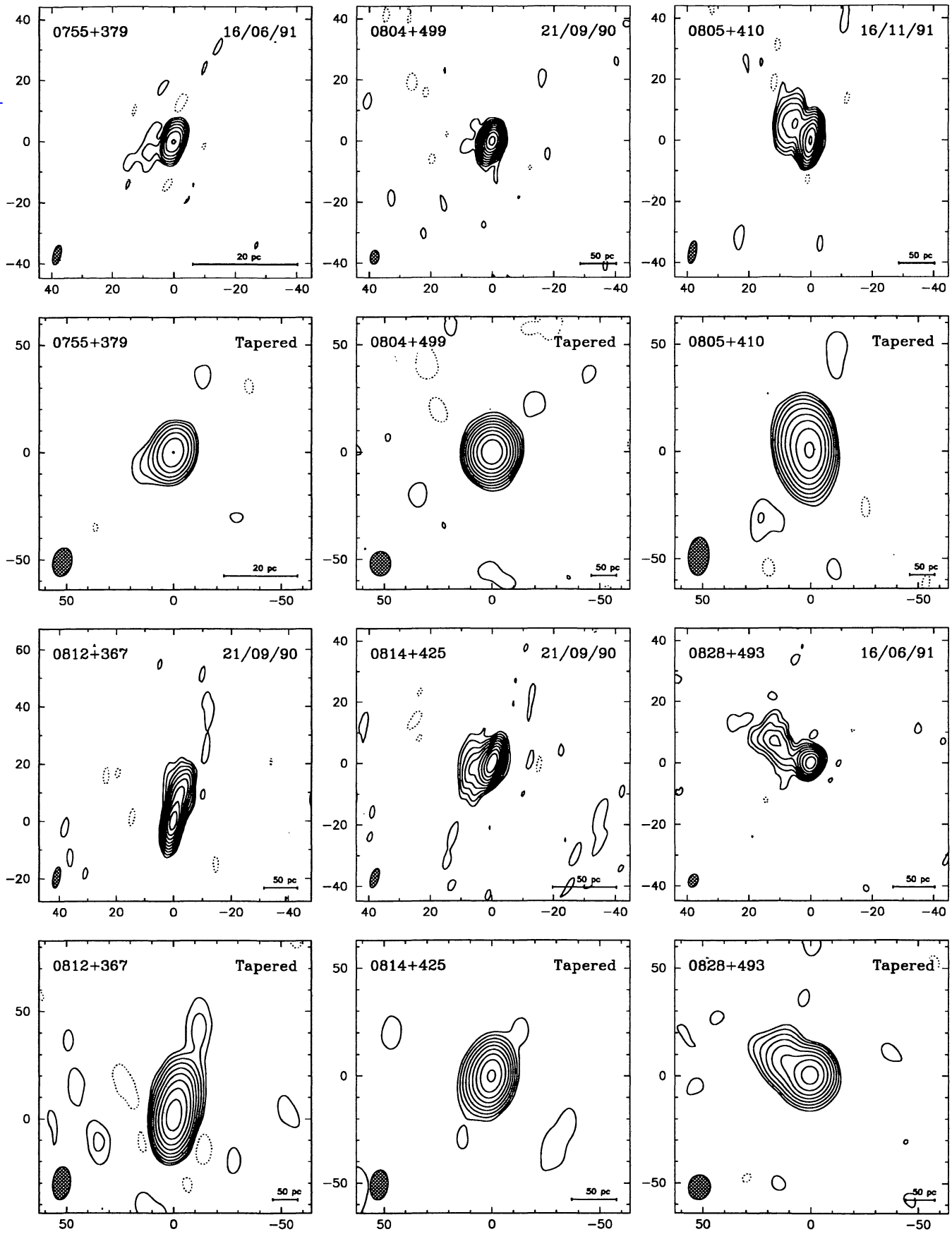

FIG. 2.—*Continued*

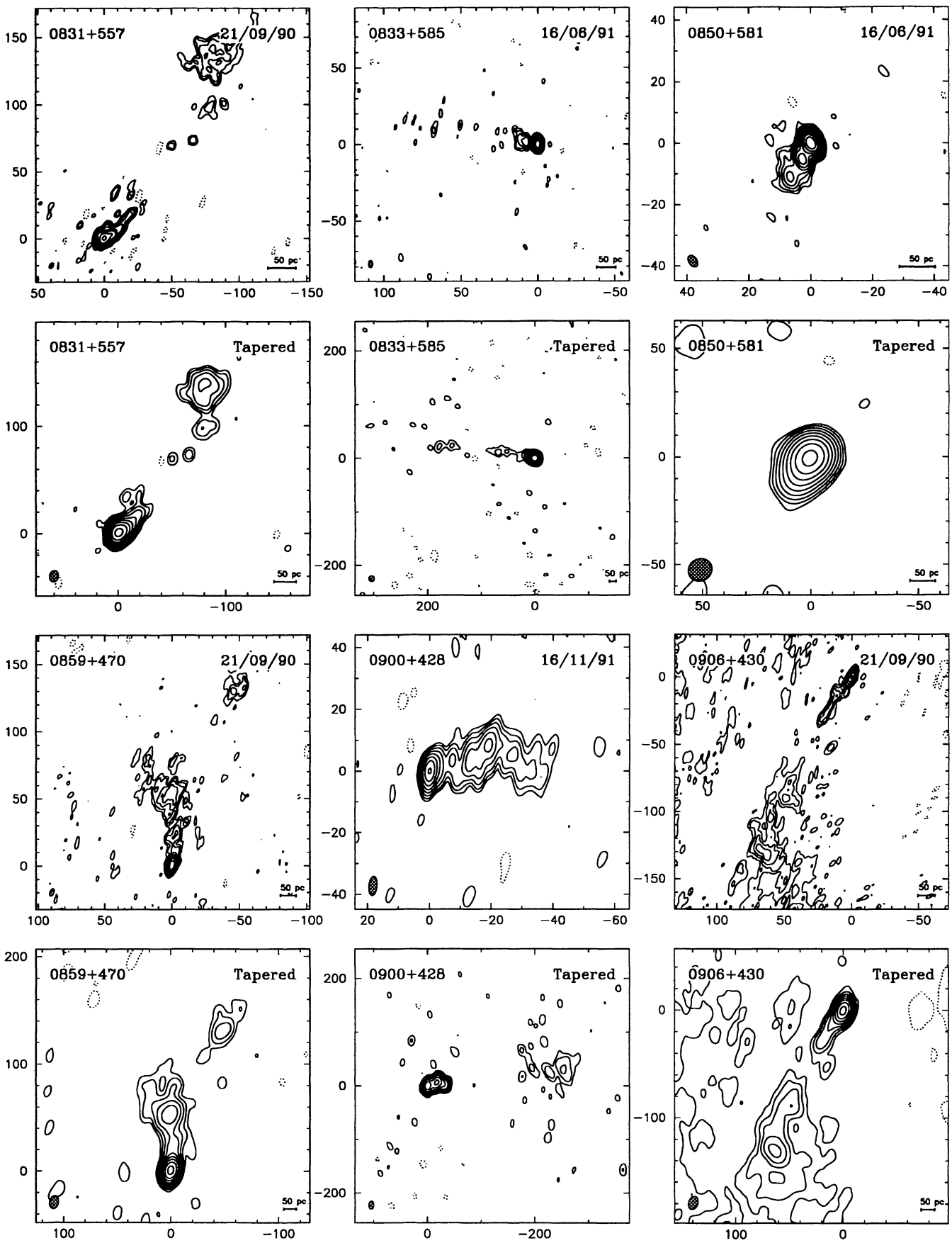

FIG. 2.—*Continued*

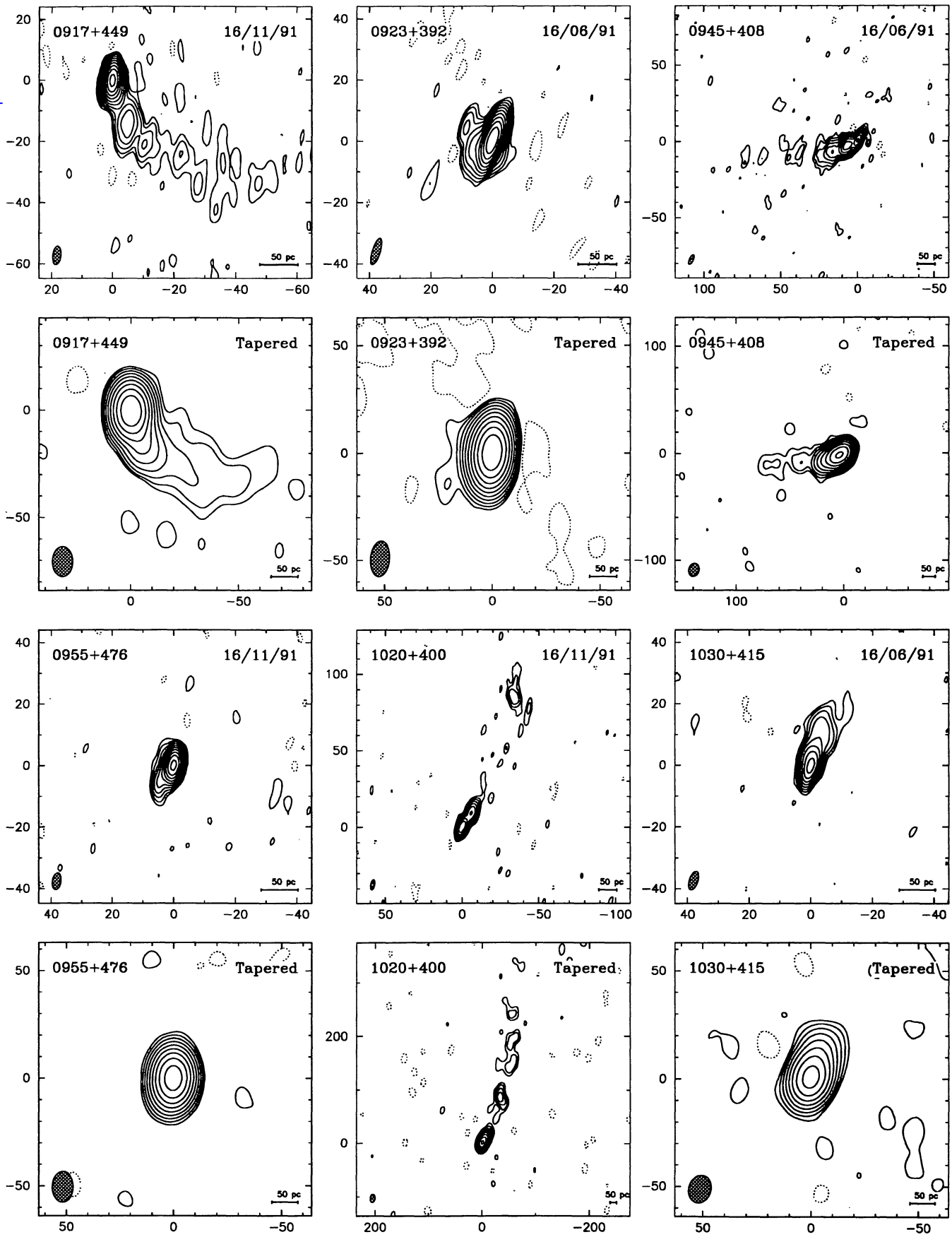

FIG. 2.—*Continued*

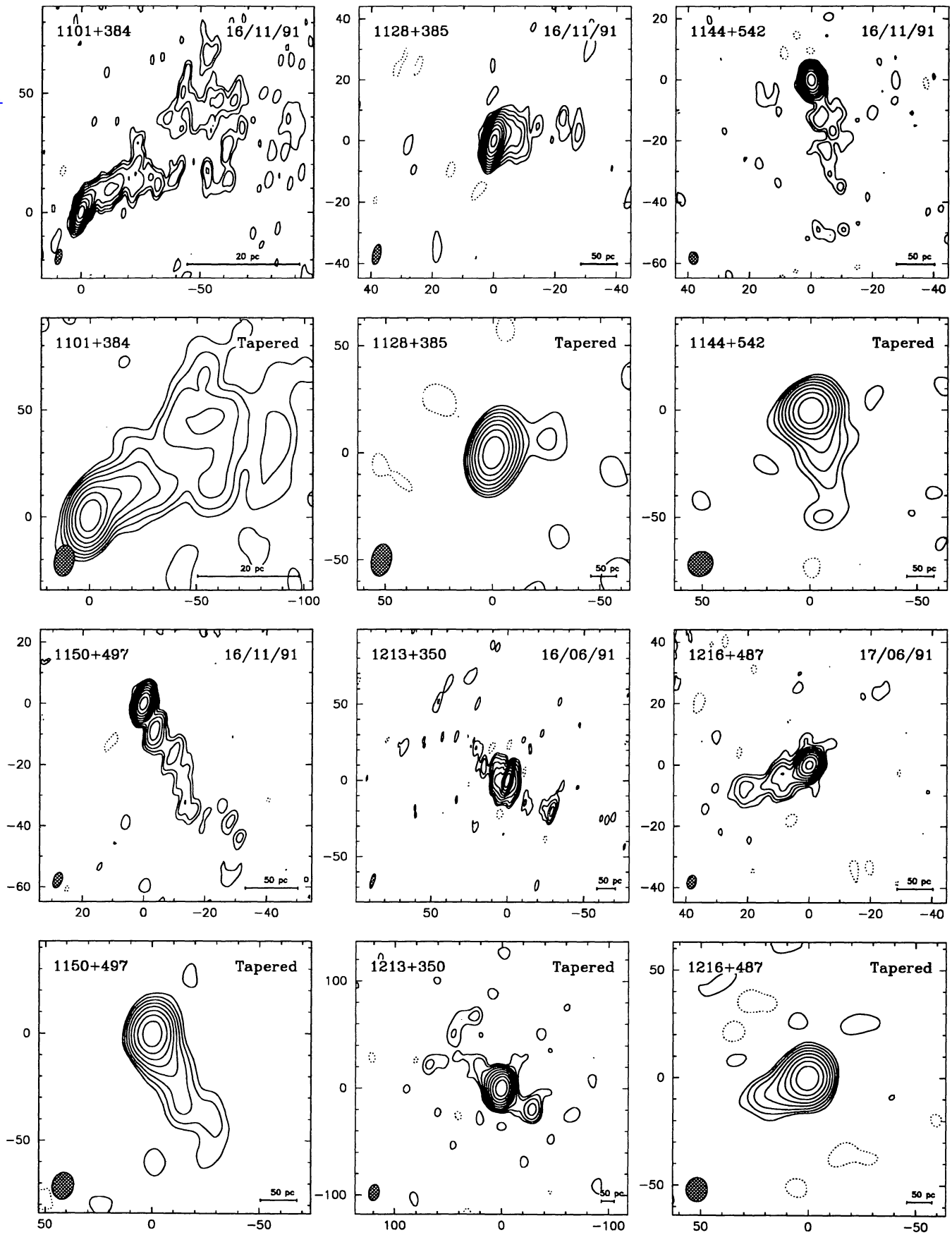

FIG. 2.—*Continued*

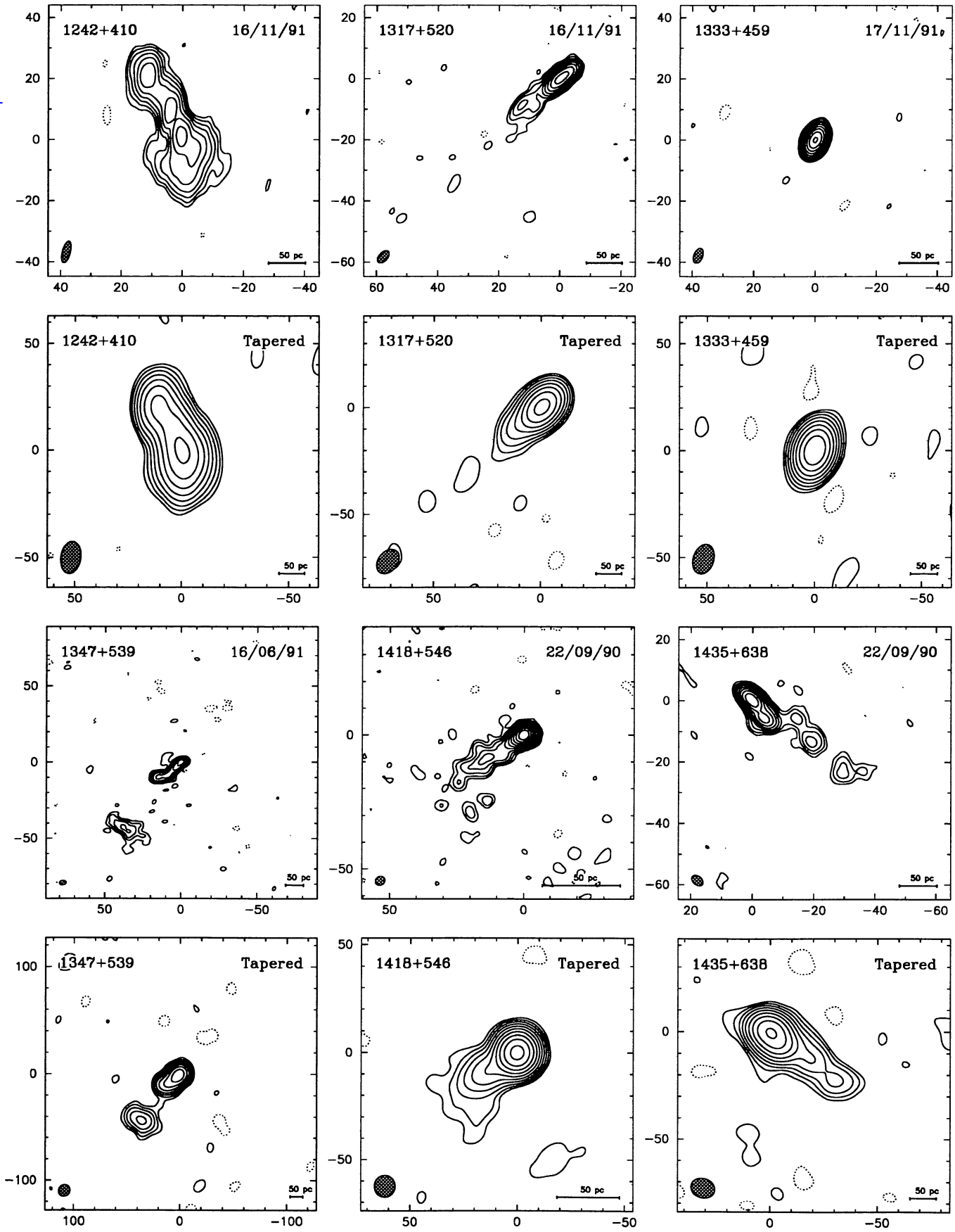

FIG. 2.—*Continued*

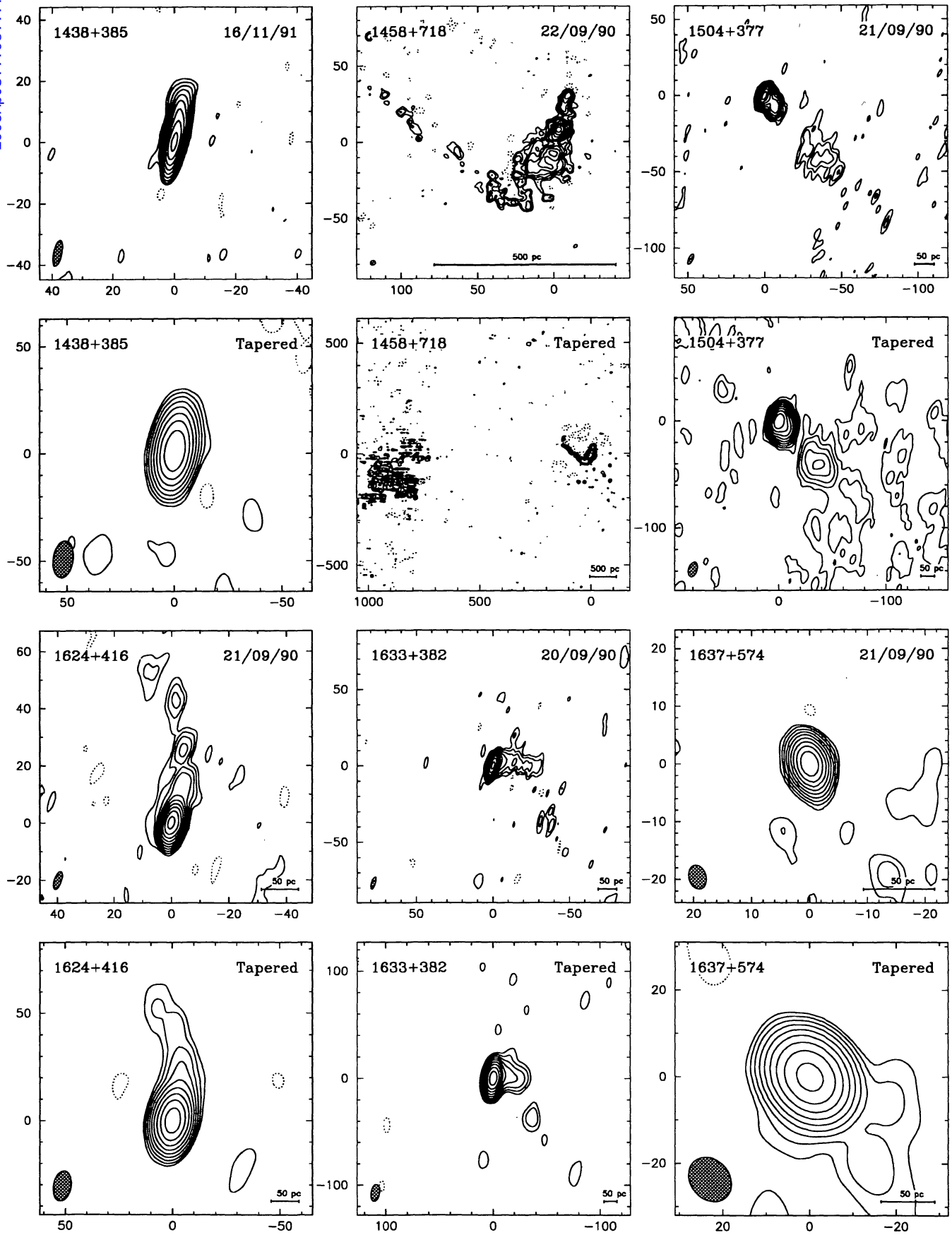

FIG. 2.—*Continued*

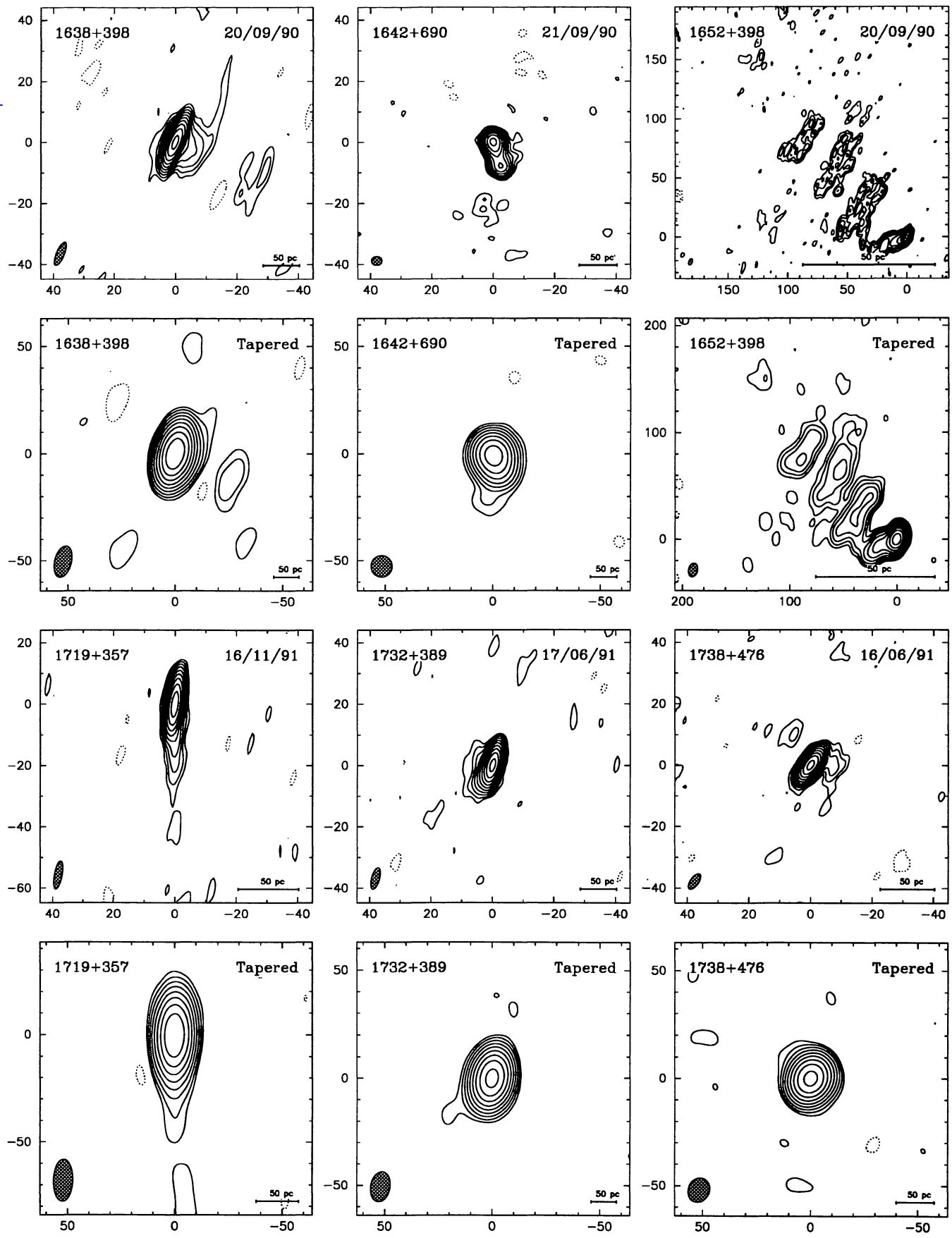

FIG. 2.—*Continued*

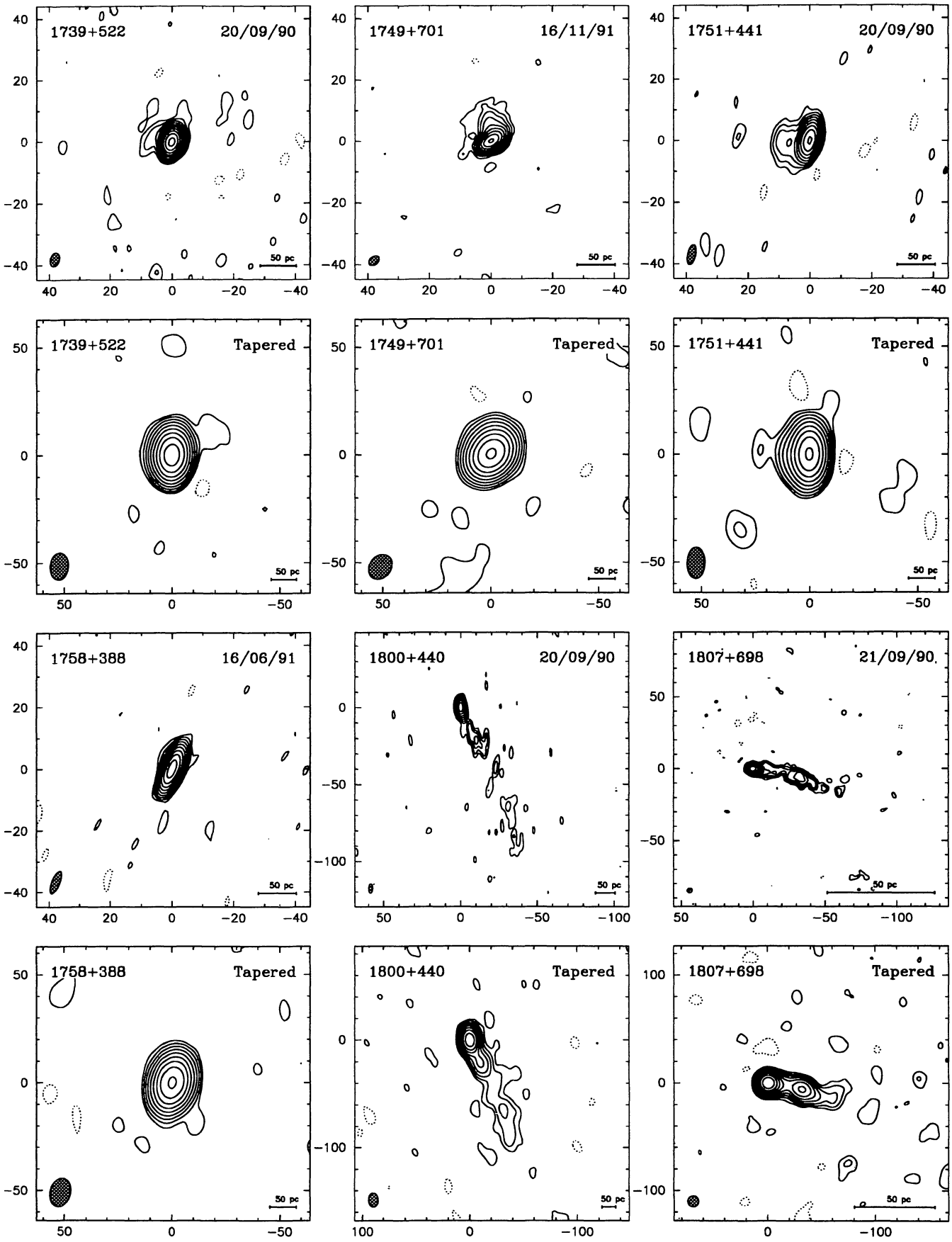

FIG. 2.—*Continued*

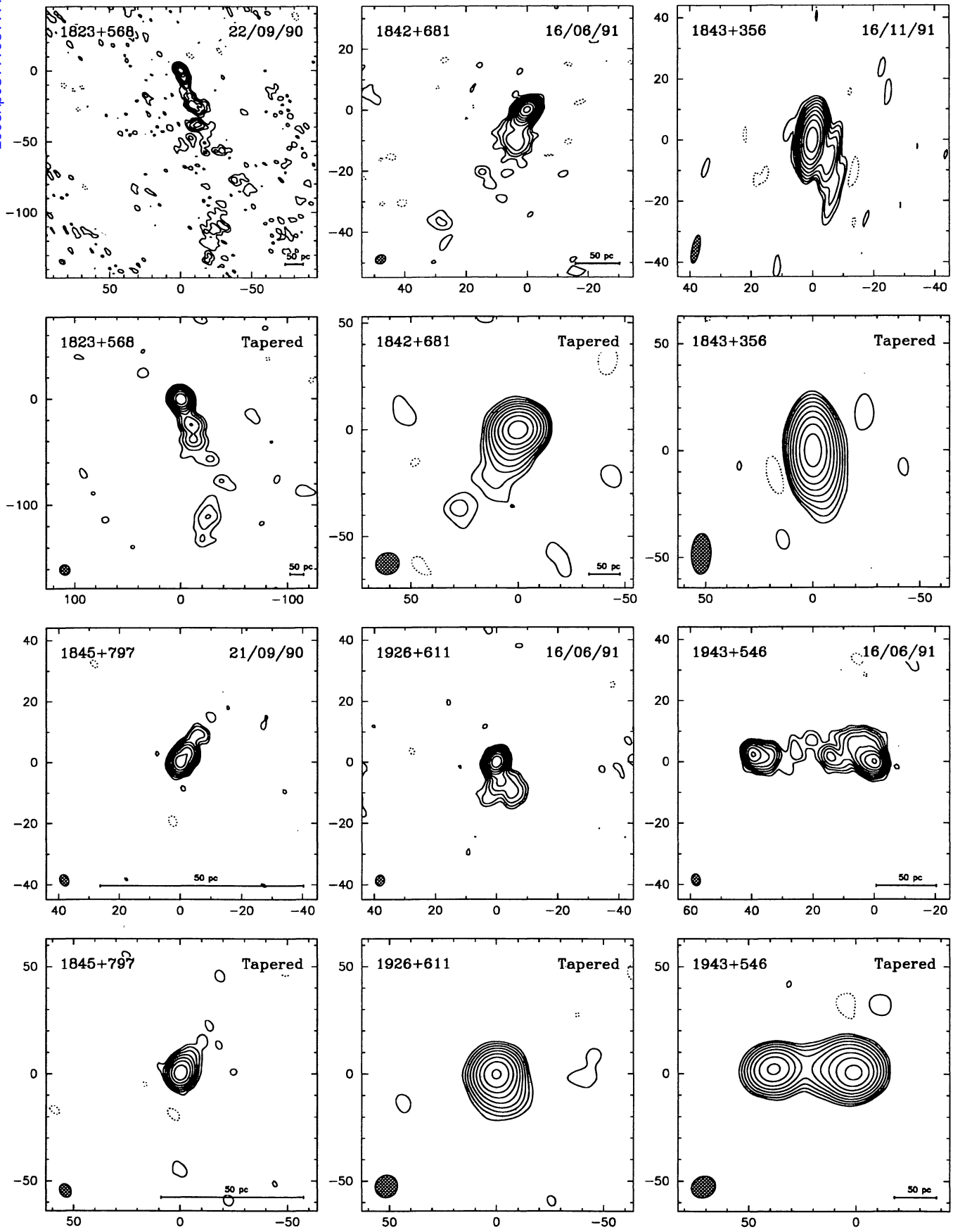

FIG. 2.—*Continued*

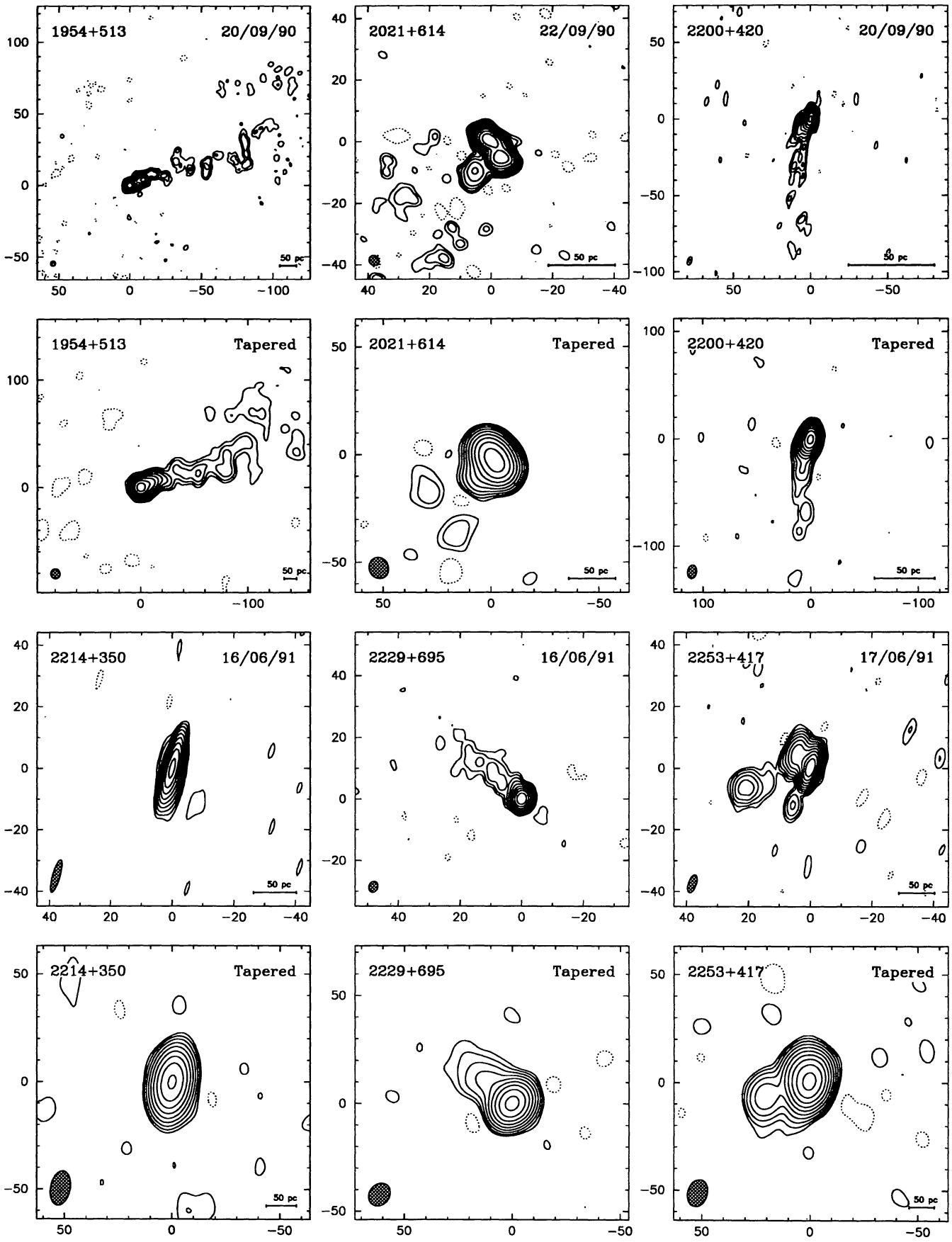

FIG. 2.—*Continued*

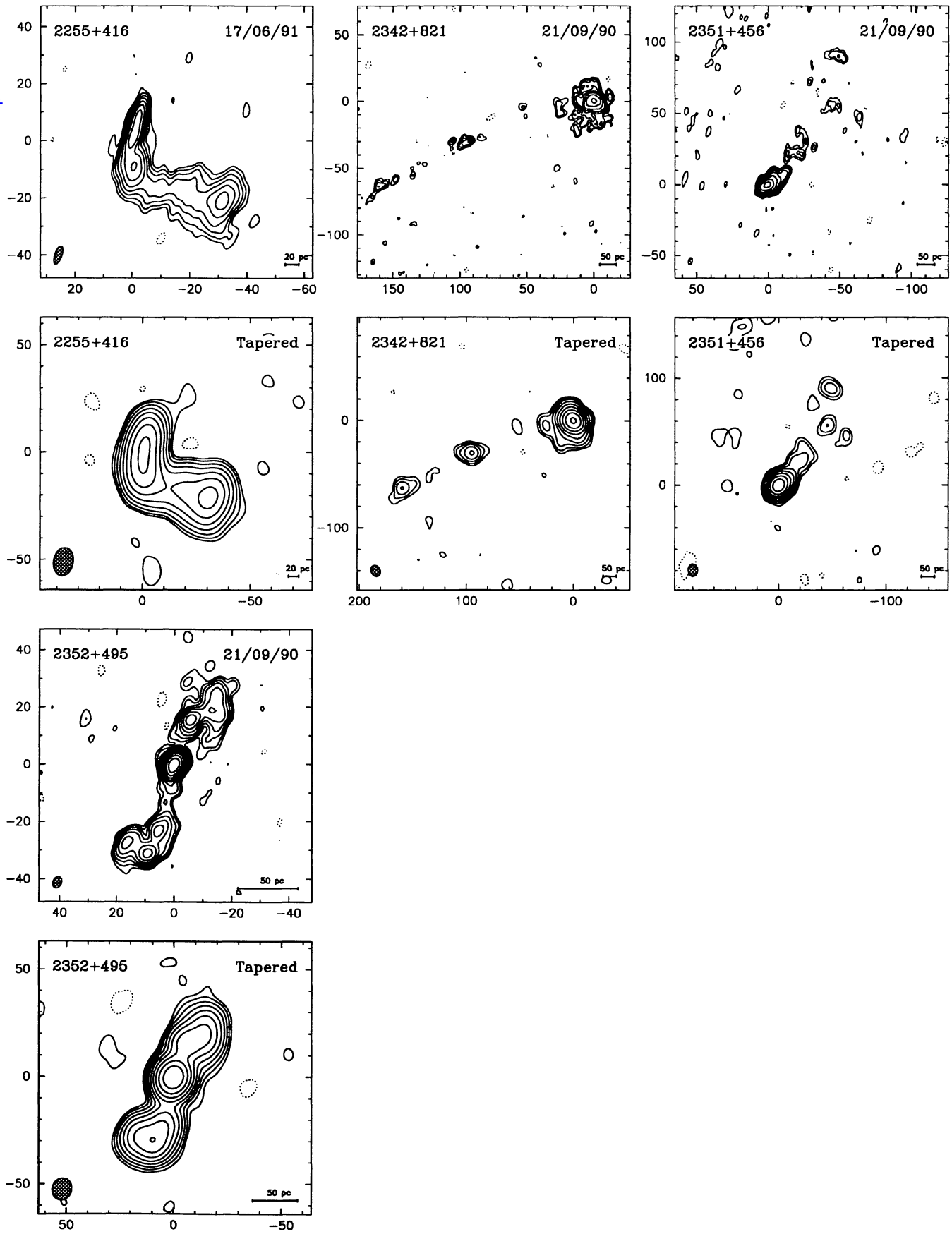

FIG. 2.—*Continued*

TABLE 4

MAP PARAMETERS

Name	Sample	Observation	Naturally Weighted Maps					Tapered Maps				
			Beam[a]			S_{peak}	rms	Beam[a]			S_{peak}	rms
			a (mas)	b (mas)	θ (°)	(mJy/beam)		a (mas)	b (mas)	θ (°)	(mJy/beam)	
0010+405...	CJ1	1990 Sep	7.10	2.56	−19	227	0.44	14.34	8.59	−13	243	0.65
0010+775...	CJ1	1991 Nov	64.50	49.19	−24	530	0.80					
0102+480...	CJ1	1991 Jun	5.60	2.55	−10	990	0.54	12.35	9.38	−5	1180	1.13
0108+388...	PR	1990 Sep	5.89	2.72	−13	249	0.59	12.59	9.08	−14	427	0.74
0133+476...	PR	1990 Sep	5.18	2.71	−24	1000	0.50	12.07	8.91	−16	1290	0.74
0218+357...	CJ1	1991 Nov	7.78	2.86	−15	79	0.35	17.21	9.67	−2	175	0.53
0248+430...	CJ1	1991 Jun	6.41	2.55	−6	593	0.57	13.04	9.12	−2	788	0.96
0402+379...	CJ1	1990 Sep	7.27	2.49	−13	165	0.68	14.63	7.96	−4	395	1.27
0404+768...	PR	1990 Sep	3.45	2.85	75	311	0.86	9.79	8.74	68	1220	0.69
0538+498...	PR	1990 Sep	4.78	2.76	−1	1070	1.40	11.10	8.90	11	2230	4.18
0602+673...	CJ1	1990 Sep	3.54	3.12	−49	479	0.35	10.48	9.86	−57	539	0.57
0620+389...	CJ1	1991 Nov	8.49	2.50	−11	390	0.30	18.62	9.40	−2	569	0.48
0642+449...	CJ1	1991 Nov	6.63	2.59	−10	268	0.25	15.92	9.58	−2	431	0.50
0711+356...	PR	1991 Jun	7.92	2.52	−16	1350	0.60	14.72	9.72	−8	1590	0.93
0716+714...	CJ1	1991 Nov	4.28	2.79	19	198	0.26	13.66	10.91	65	217	0.54
0723+679...	PR	1990 Sep	4.79	2.58	−26	161	0.33	13.35	8.98	−8	230	0.72
0740+828...	CJ1	1991 Jun	5.45	2.46	30	479	0.45	12.51	8.98	67	693	0.81
0746+483...	CJ1	1991 Nov	5.15	2.82	−5	557	0.26	13.45	9.94	0	700	0.40
0755+379...	CJ1	1991 Jun	6.67	2.50	−14	102	0.52	13.52	8.93	−13	160	0.83
0804+499...	PR	1990 Sep	4.63	2.81	−10	807	0.43	11.34	9.78	−2	912	0.66
0805+410...	CJ1	1991 Nov	17.76	9.56	−3	377	0.44	17.76	9.56	−3	377	0.44
0812+367...	CJ1	1990 Sep	7.54	2.57	−11	420	0.32	15.33	8.44	−6	521	0.47
0814+425...	PR	1990 Sep	6.55	2.58	−16	813	0.49	13.87	8.40	−7	946	1.11
0828+493...	CJ1	1991 Jun	4.43	2.95	−21	215	0.34	11.48	10.05	−10	269	0.48
0831+557...	PR	1990 Sep	4.61	2.53	−26	1230	1.50	10.76	8.02	−12	3600	3.44
0833+585...	CJ1	1991 Jun	4.69	2.59	0	628	0.40	10.91	10.40	23	727	0.50
0850+581...	PR	1991 Jun	4.21	2.65	30	643	0.41	11.24	10.17	−55	792	0.83
0859+470...	PR	1990 Sep	5.50	2.64	−21	618	0.45	12.29	8.39	−13	893	0.86
0900+428...	CJ1	1991 Nov	6.23	2.70	−6	143	0.36	15.14	9.56	−2	180	0.47
0906+430...	PR	1990 Sep	5.96	2.65	−22	320	0.40	12.61	8.51	−17	387	0.78
0917+449...	CJ1	1991 Nov	6.13	2.65	−6	700	0.35	14.03	9.49	0	790	0.48
0923+392...	PR	1991 Jun	9.07	2.61	−17	2510	0.87	16.68	8.89	−5	3040	1.16
0945+408...	PR	1991 Jun	6.67	2.60	−23	508	0.58	12.55	9.61	−16	905	1.07
0955+476...	CJ1	1991 Nov	5.50	2.77	−9	504	0.28	14.25	9.77	−1	540	0.48
1020+400...	CJ1	1991 Nov	6.66	2.64	−12	205	0.26	15.18	9.18	−7	295	0.36
1030+415...	CJ1	1991 Jun	6.24	2.71	−19	296	0.54	13.07	10.16	−18	403	0.74
1101+384...	CJ1	1991 Nov	6.62	2.69	−13	236	0.18	14.57	9.33	−10	282	0.39
1128+385...	CJ1	1991 Nov	6.70	2.69	−14	619	0.31	15.24	9.39	−12	678	0.92
1144+542...	CJ1	1991 Nov	4.10	2.94	6	261	0.24	12.15	11.06	−41	324	0.43
1150+497...	CJ1	1991 Nov	5.23	2.68	−19	306	0.27	12.70	9.83	−11	346	0.54
1213+350...	CJ1	1991 Jun	9.79	2.44	−16	867	0.53	15.16	9.49	−11	1220	0.87
1216+487...	CJ1	1991 Jun	4.39	2.87	−11	394	0.43	11.18	9.82	−5	545	0.76
1242+410...	CJ1	1991 Nov	7.28	2.57	−14	162	0.58	15.12	9.30	−8	423	0.94
1317+520...	CJ1	1991 Nov	4.92	2.80	−42	148	0.28	12.68	9.01	−39	228	0.45
1333+459...	CJ1	1991 Nov	5.13	2.87	−21	276	0.30	14.12	9.47	−17	324	0.45
1347+539...	CJ1	1991 Jun	4.23	2.91	−83	236	0.66	11.37	10.41	−40	383	1.15
1418+546...	CJ1	1990 Sep	3.70	3.28	−54	1010	0.35	10.32	9.79	0	1220	0.67
1435+638...	CJ1	1990 Sep	4.22	2.80	48	400	0.54	11.15	9.08	70	593	0.73
1438+385...	CJ1	1991 Nov	8.55	2.59	−11	344	0.34	17.25	9.21	−7	468	0.65
1458+718...	PR	1990 Sep	3.26	3.13	85	618	0.54	11.77	11.19	−53	1320	0.48
1504+377...	CJ1	1990 Sep	7.37	2.64	−24	464	0.36	14.08	7.84	−18	579	0.40
1624+416...	PR	1990 Sep	6.64	2.60	−19	900	0.52	14.17	8.36	−10	1350	1.04
1633+382...	PR	1990 Sep	8.33	2.56	−18	2060	0.99	16.13	7.91	−8	2370	1.88
1637+574...	PR	1990 Sep	4.18	2.97	16	898	0.57	11.06	8.97	39	989	0.92
1638+398...	CJ1	1990 Sep	8.25	2.53	−22	1150	0.64	14.84	7.89	−14	1240	0.80

TABLE 4—*Continued*

Name	Sample	Observation	Naturally Weighted Maps					Tapered Maps				
			Beam[a]			S_{peak}	rms	Beam[a]			S_{peak}	rms
			a (mas)	b (mas)	θ (°)	(mJy/beam)		a (mas)	b (mas)	θ (°)	(mJy/beam)	
1642+690...	PR	1990 Sep	3.44	2.99	88	481	0.50	10.01	9.93	14	741	1.23
1652+398...	PR	1990 Sep	5.83	2.81	−19	484	0.26	12.97	8.26	−12	592	0.51
1719+357...	CJ1	1990 Sep	9.31	2.51	−10	326	0.30	19.44	9.20	−1	384	0.51
1732+389...	CJ1	1991 Jun	7.21	2.54	−14	876	0.47	14.11	9.18	−10	973	0.94
1738+476...	CJ1	1991 Jun	5.89	2.62	−35	783	0.42	11.56	9.67	−23	881	0.89
1739+522...	PR	1990 Sep	4.52	2.94	−15	1020	0.53	12.51	8.55	−3	1170	0.92
1749+701...	PR	1991 Nov	3.87	2.71	−53	339	0.38	12.31	9.99	−39	496	0.56
1751+441...	CJ1	1990 Sep	6.60	2.55	−11	335	0.40	14.48	8.21	0	425	0.52
1758+388...	CJ1	1991 Jun	7.85	2.50	−22	326	0.25	13.53	9.33	−14	392	0.46
1800+440...	CJ1	1990 Sep	6.09	2.67	−2	220	0.32	13.15	8.87	2	279	0.44
1807+698...	PR	1990 Sep	3.49	3.08	−59	633	0.39	10.32	10.04	−9	838	0.56
1823+568...	PR	1990 Sep	4.45	2.94	50	449	0.33	9.90	9.37	47	518	0.71
1842+681...	CJ1	1991 Jun	3.66	2.86	−62	747	0.41	11.22	9.91	−75	859	0.77
1843+356...	CJ1	1991 Nov	9.40	2.48	−12	447	0.34	18.83	9.13	−2	771	0.60
1845+797...	PR	1990 Sep	3.81	2.84	24	148	0.41	6.57	5.16	30	183	0.51
1926+611...	CJ1	1991 Jun	3.58	2.99	−14	506	0.30	10.74	10.16	−48	583	0.65
1943+546...	CJ1	1991 Jun	3.86	2.86	12	612	0.73	11.55	9.71	−66	1060	1.03
1954+513...	PR	1990 Sep	3.70	3.26	−20	647	0.42	9.49	8.81	10	729	0.60
2021+614...	PR	1990 Sep	3.66	2.99	46	554	0.35	10.13	8.99	24	1360	1.04
2200+420...	PR	1990 Sep	5.79	2.72	−18	1440	0.68	12.72	8.23	−9	2110	0.99
2214+350...	CJ1	1991 Jun	10.97	2.41	−16	335	0.33	16.24	9.12	−10	375	0.45
2229+695...	CJ1	1991 Jun	3.64	2.94	−17	709	0.46	11.38	9.36	−38	803	0.79
2253+417...	CJ1	1991 Jun	6.01	2.56	−18	1210	0.39	12.83	9.03	−16	1460	0.80
2255+416...	CJ1	1991 Jun	6.62	2.50	−19	256	0.78	13.25	9.24	−11	519	1.13
2342+821...	PR	1990 Sep	3.87	2.70	−14	320	0.70	10.75	8.52	25	1280	1.39
2351+456...	PR	1990 Sep	5.03	2.73	−12	265	0.53	11.62	8.82	−1	702	1.10
2352+495...	PR	1990 Sep	4.08	3.01	−24	747	0.49	10.29	9.00	−18	1060	0.64

[a] The restoring beam is an elliptical gaussian with FWHM major axis a and minor axis b, with major axis at position angle θ.

Col. (1): Source name. Col. (2): Sample: PR if $S_{6\,cm} > 1.3$ Jy, CJ1 if 1.3 Jy $> S_{6\,cm} > 0.7$ Jy; there are 31 PR sources and 51 CJ1 sources. Col. (3): Date of observations. Cols. (4)–(6). The beam characteristics of the naturally weighted maps. Col. (7): The peak flux density of the naturally weighted maps (milijansky per beam). Col. (8): The rms noise in the naturally weighted maps (millijansky per beam). Cols. (9)–(11): The beam characteristics of the tapered maps. Col. (12): The peak flux density of the tapered maps (millijansky per beam). Col. (13): The rms noise in the tapered maps (millijansky per beam).

Table 4 is published in computer-readable form in the AAS CD-ROM Series, Vol. 4.

An independent estimate of the calibration was acquired by examining the ratios of baseline amplitudes at "crossing points" in the u, v plane using the Caltech program UVCROSS. A "crossing point" was assumed to exist where points of two baselines were within 3 Mλ of each other in the u, v plane. If the calibration was perfect the ratios of the amplitudes at these points would be unity.

The correction factors derived by DIFMAP and UVCROSS were usually in excellent agreement ($\leq$3%) and were therefore combined to derive an average correction factor for each telescope. Successive iterations of this procedure were performed until the correction values obtained by DIFMAP and UVCROSS were close to unity. The calibration information provided by most telescopes was good enough for this procedure to converge rapidly. In general the corrections applied to the telescope gains were less than 15% although corrections of up to 66% were occasionally found.

Finally we examined the closure phases for any obvious baseline-dependent errors. Since the calibrators are barely resolved the closure phases should be close to zero and any major deviation from zero should be examined carefully. In the 1990 September and 1991 June sessions closure phases involving WSRT differed from zero by up to 30° in some cases. This can probably be attributed to polarization contamination (Bartel et al. 1985). We discarded all data from WSRT for these two sessions.

The calibrated data were then inspected and discrepant points deleted using DIFMAP. As far as possible, editing was antenna-based; i.e., the error could be attributed to a single antenna and all baselines involving that antenna were flagged. Caution was exercised not to delete points that might result from extended structure. Most deleted points were located at the beginning of the scan when telescopes were slewing to source.

3.5. *Imaging*

The maps were made with a standard iterative self-calibration procedure (e.g., Pearson & Readhead 1984; Wilkinson 1989) implemented in the Caltech program DIFMAP (Shepherd, Pearson, & Taylor 1994). In addition to self-calibration, Fourier inversion, and deconvolution using the

TABLE 5

GAUSSIAN MODELS

Source	S (Jy)	r (mas)	θ (°)	a (mas)	b/a	Φ (°)	χ^2
0010+405...CJ1	0.241	0.00	0.0	1.45	0.30	−54.8	1.067
	0.008	7.30	−29.5	4.84	0.30	−68.1	
0102+480...CJ1	1.136	0.00	0.0	1.78	0.69	12.3	0.835
	0.081	3.19	30.2	2.87	0.00	60.0	
	0.035	9.79	45.4	8.97	0.39	−58.0	
0108+388...PR	0.297	0.00	0.0	1.91	0.58	71.6	1.048
	0.271	5.66	75.5	2.56	0.60	−51.6	
0133+476...PR	1.226	0.00	0.0	2.78	0.45	−13.8	1.042
	0.085	4.06	−53.8	5.08	0.15	18.7	
	0.153	6.96	−7.5	9.75	0.50	−74.5	
	0.036	20.01	−36.2	33.05	0.08	−17.7	
0218+357...CJ1	0.309	0.00	0.0	21.36	0.40	−26.8	1.531
	0.259	10.74	−16.9	36.31	0.51	−57.8	
	0.113	154.12	77.4	154.34	0.48	58.0	
	0.199	334.58	67.4	7.44	0.48	73.0	
	0.113	358.95	69.6	114.21	0.57	−53.0	
0248+430...CJ1	0.691	0.00	0.0	1.51	0.93	81.3	1.072
	0.138	4.57	139.0	3.40	0.34	−41.5	
	0.207	11.03	142.4	2.19	0.40	48.9	
0602+673...CJ1	0.517	0.00	0.0	1.31	0.68	71.9	0.895
	0.050	4.25	177.9	11.49	0.27	68.4	
0620+389...CJ1	0.388	0.00	0.0	0.83	0.80	−21.4	0.969
	0.102	3.43	116.8	7.93	0.00	−49.9	
	0.187	6.49	135.7	2.52	0.62	−38.6	
	0.077	20.07	108.4	16.02	0.43	56.6	
0642+449...CJ1	0.289	0.00	0.0	1.30	0.00	81.0	1.032
	0.178	3.16	87.9	1.51	0.75	69.9	
0711+356...PR	0.841	0.00	0.0	1.38	0.00	64.6	0.881
	0.842	2.00	156.6	6.02	0.00	−23.5	
0716+714...CJ1	0.201	0.00	0.0	1.62	0.00	10.0	1.038
	0.035	5.71	17.1	9.84	0.30	24.2	
0723+679...PR	0.161	0.00	0.0	1.47	0.00	−83.3	1.126
	0.087	2.80	−87.2	2.72	0.34	−65.3	
0740+828...CJ1	0.335	0.00	0.0	1.77	0.43	−3.2	0.941
	0.351	2.26	−6.6	1.38	0.65	−24.9	
	0.146	8.05	−4.1	4.87	0.50	5.8	
	0.097	19.27	−10.0	8.99	0.55	−16.4	
	0.021	37.37	−9.6	14.72	0.39	−71.2	
0746+483...CJ1	0.452	0.00	0.0	0.90	0.34	−66.3	0.788
	0.267	1.60	−96.5	3.56	0.28	87.5	
	0.026	6.25	−93.7	4.15	0.00	−52.8	
	0.014	44.46	−99.8	35.36	0.21	80.6	
0755+379...CJ1	0.167	0.00	0.0	3.31	0.00	−89.4	1.324
	0.010	11.78	111.7	22.83	0.00	−62.6	
0804+499...PR	0.827	0.00	0.0	1.14	0.69	−53.9	0.882
	0.108	2.49	142.2	3.39	0.51	3.6	
0805+410...CJ1	0.331	0.00	0.0	2.12	0.63	5.1	1.123
	0.119	7.67	44.6	6.00	0.16	89.4	
0812+367...CJ1	0.469	0.00	0.0	3.12	0.27	−12.7	0.958
	0.161	9.70	−14.3	4.77	0.49	−30.1	
	0.016	13.37	−1.8	5.46	0.00	24.9	

TABLE 5—*Continued*

Source	S (Jy)	r (mas)	θ (°)	a (mas)	b/a	Φ (°)	χ^2
0814+425...PR	0.709	0.00	0.0	1.21	0.46	−35.1	0.978
	0.261	1.36	107.2	4.19	0.63	−49.0	
	0.062	6.63	101.6	6.74	0.39	−38.4	
0828+493...CJ1	0.230	0.00	0.0	1.29	0.29	70.1	1.020
	0.043	2.76	55.6	1.35	0.38	75.9	
	0.079	12.82	60.8	9.90	0.49	41.3	
0833+585...CJ1	0.714	0.00	0.0	1.53	0.45	80.9	1.178
	0.071	7.86	77.6	8.38	0.52	63.2	
0850+581...PR	0.712	0.00	0.0	1.40	0.55	−24.3	0.995
	0.171	6.00	152.7	2.46	0.00	−32.1	
	0.058	12.35	146.5	8.74	0.17	6.0	
0900+428...CJ1	0.178	0.00	0.0	2.50	0.57	−17.0	1.476
	0.021	8.92	−63.5	8.12	0.00	6.2	
	0.103	15.34	−79.4	12.04	0.48	−51.5	
	0.059	20.96	−65.8	3.13	0.29	−67.6	
	0.045	30.30	−85.2	12.20	0.51	59.8	
	0.061	252.21	−83.0	53.35	0.68	−12.1	
0917+449...CJ1	0.747	0.00	0.0	1.53	0.43	−4.9	0.975
	0.062	4.49	−158.0	2.57	0.93	−11.4	
	0.072	15.58	−161.1	8.61	0.38	−4.3	
	0.009	24.09	−156.0	2.46	0.00	−53.6	
	0.049	32.92	−138.5	40.06	0.27	59.8	
0923+392...PR	2.854	0.00	0.0	1.71	0.34	−87.2	1.168
	0.348	2.71	84.5	9.24	0.13	−59.9	
	0.021	5.95	−145.9	10.92	0.00	−28.9	
	0.010	8.59	68.2	12.85	0.00	−20.3	
0945+408...PR	0.518	0.00	0.0	1.16	0.00	−77.2	1.354
	0.837	7.94	117.5	5.52	0.54	−77.9	
	0.179	19.23	114.5	7.51	0.88	−57.4	
	0.076	41.77	102.4	59.14	0.23	−86.7	
0955+476...CJ1	0.516	0.00	0.0	0.99	0.58	−23.6	0.830
	0.043	4.54	132.8	8.54	0.19	−23.9	
1020+400...CJ1	0.185	0.00	0.0	2.38	0.27	−31.0	1.125
	0.098	2.88	−45.0	1.60	0.00	−32.3	
	0.117	11.63	−35.1	6.56	0.44	−27.7	
	0.062	90.08	−21.5	85.59	0.15	−4.7	
1030+415...CJ1	0.280	0.00	0.0	1.57	0.45	5.5	1.141
	0.131	3.54	2.7	2.98	0.62	68.5	
	0.086	11.83	−17.2	8.64	0.59	3.2	
1101+384...CJ1	0.224	0.00	0.0	0.73	0.00	−66.9	0.901
	0.064	3.04	−37.9	8.99	0.17	−31.0	
	0.090	17.59	−53.0	21.50	0.32	−60.5	
	0.103	64.45	−53.8	49.29	0.73	3.3	
1128+385...CJ1	0.627	0.00	0.0	1.21	0.52	5.3	1.084
	0.068	2.76	−66.2	6.21	0.65	−32.1	
	0.030	11.48	−81.4	21.33	0.47	−65.4	
1144+542...CJ1	0.315	0.00	0.0	2.32	0.48	12.1	1.028
	0.019	3.44	−158.4	7.96	0.00	−61.6	
	0.032	17.11	−161.4	22.84	0.55	10.6	
1150+497...CJ1	0.337	0.00	0.0	1.71	0.21	19.6	1.019
	0.030	9.48	−158.6	4.35	0.51	−6.4	
	0.046	23.16	−152.9	40.62	0.11	24.0	
1213+350...CJ1	0.959	0.00	0.0	1.77	0.83	32.7	1.373
	0.173	3.23	−150.2	8.01	0.66	72.0	
	0.369	4.73	95.5	11.56	0.43	27.5	
	0.031	35.58	−125.6	2.67	0.59	−55.4	

TABLE 5—*Continued*

Source	S (Jy)	r (mas)	θ (°)	a (mas)	b/a	Φ (°)	χ^2
1216+487...CJ1	0.509	0.00	0.0	2.64	0.36	−76.6	1.326
	0.099	5.17	116.2	8.22	0.31	−77.3	
	0.043	16.34	116.7	15.38	0.24	87.2	
1242+410...CJ1	0.286	0.00	0.0	6.46	0.48	6.2	1.288
	0.271	7.44	−145.2	6.87	0.59	−25.0	
	0.225	8.63	23.8	3.53	0.89	88.2	
	0.117	13.11	174.1	8.74	0.43	61.4	
	0.268	22.12	28.1	4.49	0.84	44.3	
1317+520...CJ1	0.255	0.00	0.0	6.32	0.16	−51.1	1.392
	0.004	8.00	109.3	13.17	0.00	−19.8	
	0.019	15.55	123.6	22.19	0.00	−10.3	
1333+459...CJ1	0.330	0.00	0.0	2.12	0.51	−64.6	1.033
1347+539...CJ1	0.218	0.00	0.0	1.64	0.76	−40.9	1.459
	0.199	4.06	137.3	5.92	0.00	−38.4	
	0.194	14.63	130.3	10.73	0.29	−78.0	
	0.126	57.30	140.2	14.72	0.44	49.8	
1418+546...CJ1	0.931	0.00	0.0	1.10	0.00	−54.4	0.946
	0.347	1.82	130.4	4.64	0.36	−64.3	
	0.112	17.07	122.9	16.43	0.00	−66.2	
1435+638...CJ1	0.558	0.00	0.0	3.74	0.35	43.0	1.142
	0.214	7.09	−146.7	2.32	0.77	72.5	
	0.071	19.83	−120.8	14.02	0.20	31.1	
	0.025	39.26	−128.7	5.33	0.46	−40.7	
1438+385...CJ1	0.423	0.00	0.0	4.53	0.29	−14.6	1.535
	0.119	9.12	−11.1	4.68	0.00	23.2	
1504+377...CJ1	0.499	0.00	0.0	1.39	0.66	54.4	0.918
	0.109	3.25	−132.1	3.14	0.68	−36.9	
	0.176	9.85	−135.2	6.62	0.25	31.6	
	0.077	54.87	−137.5	25.39	0.49	47.8	
1624+416...PR	0.859	0.00	0.0	1.63	0.45	63.5	1.092
	0.392	0.98	−52.4	6.28	0.51	−5.1	
	0.184	2.64	−136.6	2.81	0.00	−37.9	
	0.109	18.19	−11.0	25.03	0.24	−0.2	
1633+382...PR	1.855	0.00	0.0	0.98	0.49	43.5	1.419
	0.548	1.57	−63.6	3.10	0.00	85.3	
	0.296	12.29	−77.7	24.12	0.43	85.8	
	0.042	53.64	−135.0	15.90	0.61	18.1	
1637+574...PR	0.994	0.00	0.0	1.86	0.42	17.8	0.999
	0.050	10.38	−145.7	28.30	0.66	77.2	
1638+398...CJ1	1.186	0.00	0.0	0.89	0.49	61.6	0.922
	0.108	2.87	−116.4	9.25	0.00	75.8	
1642+690...PR	0.450	0.00	0.0	1.69	0.30	1.3	1.094
	0.307	2.54	−165.0	3.46	0.26	12.4	
	0.146	8.43	−163.3	2.76	0.41	9.7	
	0.010	22.39	173.1	4.80	0.53	−33.6	
1652+398...PR	0.439	0.00	0.0	2.25	0.18	−27.8	1.484
	0.163	2.43	117.1	4.40	0.00	−63.8	
	0.202	14.22	114.8	24.31	0.17	−58.7	
	0.180	41.46	57.3	44.19	0.38	−17.9	
	0.220	95.70	44.0	72.15	0.83	−5.6	
1719+357...CJ1	0.390	0.00	0.0	5.30	0.09	−1.5	0.925
	0.020	13.28	−178.1	13.06	0.14	−3.2	

TABLE 5—*Continued*

Source	S (Jy)	r (mas)	θ (°)	a (mas)	b/a	Φ (°)	χ^2
1732+389...CJ1	0.862	0.00	0.0	0.78	0.65	70.8	1.057
	0.138	2.38	121.7	4.53	0.43	−44.2	
1738+476...CJ1	0.803	0.00	0.0	1.29	0.85	−40.1	1.024
	0.090	1.43	−69.4	2.63	0.51	43.8	
	0.019	7.25	−99.3	12.44	0.22	−14.1	
1739+522...PR	1.133	0.00	0.0	1.37	0.88	79.0	1.042
	0.074	2.56	8.5	7.80	0.21	−75.1	
1749+701...PR	0.449	0.00	0.0	3.05	0.37	−59.7	1.156
	0.088	3.55	−25.3	6.66	0.36	56.5	
	0.012	8.17	−3.2	2.34	0.00	18.3	
1751+441...CJ1	0.329	0.00	0.0	1.53	0.05	−73.1	0.967
	0.095	1.69	70.8	2.70	0.16	−39.7	
	0.038	6.61	84.0	8.20	0.53	−80.7	
1758+388...CJ1	0.333	0.00	0.0	1.19	0.71	73.1	0.999
	0.066	1.71	−91.4	1.61	0.56	−55.7	
1800+440...CJ1	0.181	0.00	0.0	1.70	0.00	33.1	1.136
	0.096	1.57	−134.3	4.09	0.22	19.4	
	0.084	25.98	−153.1	50.02	0.15	29.0	
1807+698...PR	0.632	0.00	0.0	1.88	0.25	87.9	1.346
	0.263	2.53	−98.3	4.79	0.11	81.8	
	0.274	28.15	−101.7	31.30	0.19	73.5	
	0.041	33.06	−96.9	2.99	0.66	60.2	
1823+568...PR	0.494	0.00	0.0	1.54	0.44	15.4	0.962
	0.081	5.52	−160.2	4.00	0.00	14.1	
	0.056	27.41	−159.9	9.29	0.57	47.8	
	0.025	39.06	−163.9	4.15	0.51	−77.4	
	0.046	112.96	−169.2	41.06	0.71	−16.6	
1842+681...CJ1	0.668	0.00	0.0	1.07	0.09	−20.1	0.992
	0.168	1.29	121.9	1.64	0.00	−6.2	
	0.036	4.29	149.3	2.79	0.54	−64.2	
	0.067	10.38	157.9	6.82	0.77	4.8	
1843+356...CJ1	0.807	0.00	0.0	4.54	0.43	32.3	1.022
	0.054	7.81	−134.5	4.86	0.00	−31.8	
	0.010	20.75	−163.3	14.25	0.17	−14.7	
1845+797...PR	0.156	0.00	0.0	2.02	0.00	−44.9	0.972
	0.070	3.75	−39.9	1.86	0.00	−19.8	
	0.048	5.96	−36.0	19.32	0.12	−37.2	
1926+611...CJ1	0.562	0.00	0.0	1.49	0.55	−45.4	1.035
	0.092	7.19	−163.4	9.44	0.39	46.8	
1943+546...CJ1	0.518	0.00	0.0	1.71	0.65	58.4	1.186
	0.468	2.25	84.5	3.39	0.48	83.6	
	0.125	6.08	70.1	9.95	0.00	−68.2	
	0.259	7.71	40.4	8.26	0.56	89.6	
	0.063	15.03	82.8	1.79	0.44	−82.5	
	0.016	23.04	75.1	4.09	0.00	25.8	
	0.216	35.94	87.5	6.20	0.56	−68.3	
	0.344	40.08	86.3	1.74	0.62	85.1	
2200+420...PR	1.053	0.00	0.0	6.56	0.48	−26.2	1.380
	1.306	2.07	−28.0	3.29	0.00	13.0	
	0.127	7.79	129.0	9.69	0.18	−21.8	
	0.093	24.95	168.1	27.85	0.24	−16.5	
	0.019	66.47	176.8	14.05	0.00	35.6	
2214+350...CJ1	0.277	0.00	0.0	1.63	0.00	−17.9	0.998
	0.110	1.96	−173.2	5.11	0.33	13.4	

TABLE 5—*Continued*

Source	S (Jy)	r (mas)	θ (°)	a (mas)	b/a	Φ (°)	χ^2
2229+695...CJ1	0.711	0.00	0.0	0.98	0.67	−81.0	0.921
	0.105	1.35	23.2	4.80	0.00	21.4	
	0.011	6.07	43.0	9.87	0.18	13.2	
	0.059	15.67	49.7	16.24	0.35	54.7	
2253+417...CJ1	1.334	0.00	0.0	2.02	0.45	−6.6	1.203
	0.322	5.67	41.4	4.71	0.50	43.2	
	0.013	12.70	152.7	2.65	0.51	22.2	
	0.078	21.70	108.3	5.96	0.67	−73.9	
2255+416...CJ1	0.277	0.00	0.0	9.34	0.48	−23.4	1.744
	0.423	11.00	76.4	22.94	0.35	76.6	
	0.033	28.29	71.6	2.08	0.00	45.9	
	0.429	33.38	69.4	7.07	0.60	31.2	
	0.397	38.37	54.1	4.76	0.37	−19.7	
	0.222	41.98	44.0	2.86	0.26	−7.8	
2352+495...PR	0.820	0.00	0.0	3.01	0.70	−36.0	1.683
	0.322	1.52	164.8	3.38	0.00	−16.0	
	0.057	12.92	−26.8	19.64	0.00	−29.5	
	0.221	16.71	−20.2	3.11	0.53	−58.9	
	0.092	22.41	174.2	23.41	0.00	−12.5	
	0.137	24.15	166.5	4.14	0.26	−22.5	
	0.285	24.53	−36.2	11.99	0.45	−7.7	
	0.181	32.07	150.6	5.11	0.78	85.9	
	0.205	32.33	163.2	3.86	0.00	68.1	

NOTES.—Table reports parameters of each Gaussian component of the model brightness distribution: S, flux density; r, θ, polar coordinates of the center of the component relative to an arbitrary origin, with polar angle measured from north through east; a, b, major and minor axes of the FWHM contour; Φ, position angle of the major axis measured from north through east. The sources 0010+775, 0402+379, 0404+768, 0538+498, 0831+557, 0859+470, 0906+430, 1458+718, 1954+513, 2021+614, 2342+821, and 2351+456 were too complicated to model.

Table 5 is published in computer-readable form in the AAS CD-ROM Series, Vol. 4.

CLEAN algorithm, DIFMAP incorporates data editing, display, and model fitting. In the self-calibration step, antenna phase solutions were determined with a 1 minute interval, and antenna amplitude solutions were determined with a 1 minute interval for sources stronger than 500 mJy or a 30 minute interval for weaker sources.

For each source we made several maps using different weighting and tapering of the visibility data. In Figure 2, we present two maps for each source. The first is a "naturally weighted" map, in which each measured visibility is weighted by the inverse square-root of its estimated variance. This weighting gives better results than using weighting by inverse variance, which overemphasizes the few high-sensitivity antennas and tends to give high sidelobe responses. The interferometer baselines range from 0.3 to 55 Mλ giving a minimum restoring beamwidth of ~3 mas (FWHM). However, at declinations near our southern limit of 35° the beam is elongated by about a factor of 3. In order to detect any additional low-brightness components located away from the center of the map we also mapped a field 1″ square using natural weighting with an additional Gaussian taper dropping to 20% at baseline 20 Mλ. In these maps the FWHM beamwidth is typically ~10 mas. In Figure 2 we present only the central part of the field of view where significant emission was detected.

The restoring beam, peak brightness, and rms noise for each of the maps presented in Figure 2 are given in Table 4. All the maps are convolved with the "formal beam" (an estimate of the FWHM of the central lobe of the dirty map) which is calculated in DIFMAP from the second moments of the visibility weighting function. In the majority of the maps the dynamic range is limited by thermal noise; the typical rms noise (σ) in the naturally weighted images away from the source is ~0.5–1 mJy beam^{-1}. As the core strength is usually a few hundred mJy the dynamic range in the maps is typically a few hundred-to-one. In general the rms noise is lower in the maps made from the 1991 June observations, which had the largest number of telescopes.

3.6. *Model Fitting*

Quantitative parameters of the source brightness distributions were estimated by fitting elliptical Gaussian models to the real and imaginary parts of the self-calibrated visibility data using a nonlinear least-squares algorithm in DIFMAP. The quality of the agreement between the model and the visibilities is expressed in the form of reduced χ^2: a value close to unity indicates that the model is an accurate representation of the data (although not necessarily a unique one).[3] On the whole,

[3] χ^2 is the sum of the squares of the deviations between the model and the measured visibilities, normalized by the errors estimated from the scatter in the data within a coherent integration. Reduced χ^2 is χ^2 divided by the number of degrees of freedom, here taken to be twice the number of visibilities (for independent real and imaginary parts). This is an overestimate of the number of degrees of freedom, because a small number of model parameters and a larger number of antenna calibration parameters have been estimated from the data.

most of the structures observed in the survey were simple and reduced χ^2 values close to unity were obtained with simple models comprised of a few Gaussian components. For complicated sources model fitting is very time-consuming and of limited utility; for these sources no models are presented.

The models are listed in Table 5. For multicomponent models the center of the most compact component was chosen as the coordinate origin. Comparisons with the λ-6 cm models (PR88; Xu et al. 1995) show that this component usually has a flat or inverted spectrum and can thus be identified with the optically thick core.

4. CONCLUSION

In this first paper of the series we have defined the sample of sources studied in the first Caltech–Jodrell Bank VLBI survey (CJ1). The complete sample of 135 sources is listed in Table 1. We have shown that we can make reliable images using Mark II VLBI in an efficient "snapshot" mode, and have reported on λ-18 cm snapshot observations of 56 of the CJ1 sources and 31 sources from the PR sample (Table 2). From these observations we were able to make images of 51 CJ1 sources and 31 PR sources (Table 4 and Fig. 2), and Gaussian models of 49 CJ1 sources and 21 PR sources (Table 5).

Observations at λ-18 cm of a further 25 sources are presented in Paper II (Thakkar et al. 1995), which completes the λ-18 cm part of the CJ1 survey. In addition, we have made higher resolution λ-6 cm observations of 87 CJ1 sources, which will be presented in Paper III (Xu et al. 1995). The interpretation of the results from the CJ1 survey will be given in later papers in the series.

We thank the staffs at the observations in the European and the U.S. VLBI Networks for their efforts during the CJ1 survey. We also thank Dr. Leonid Matveyenko and the staffs of the telescopes in the former Soviet Union who made special efforts to participate in these observations. A. G. P. acknowledges the receipt of a British Council Fellowship for the year 1991. The work at the California Institute of Technology was supported by the National Science Foundation (grants AST-8814554 and AST-9117100). Some of the data in Table 1 were obtained by way of the NASA/IPAC Extragalactic Database (NED), which is operated by the Jet Propulsion Laboratory, Caltech, under contract with the National Aeronautics and Space Administration. We are grateful to the referee, Margo Aller, for helpful comments.

APPENDIX
FIDELITY AND RELIABILITY OF SNAPSHOT IMAGES

It is important to demonstrate that the images are of a sufficient quality for classification purposes. Even for perfectly calibrated data, "reconstruction" errors are present on-source, arising from the inability of the deconvolution algorithms to interpolate over unsampled regions of the u, v plane. In addition the surface brightness sensitivity of any array is limited and hence weak extended features can be missed.

In 1990 September we observed the well-known sources 0538+498 (3C 147), 1458+718 (3C 309.1), and 1807+698 (3C 371) as a direct test of the reliability of the images produced by snapshot observations. For 0538+498 and 1458+718 maps made from full track observations at λ-18 cm with 10 and 8 stations, respectively, were available for comparison (Simon, Readhead, & Wilkinson 1984; Wilkinson et al. 1984). For 1807+698 a 12 station map made at λ-6 cm was available (Lind 1987). All three sources have core-jet structures in which the jet has complex substructure. The comparisons between the full-track maps and our snapshot maps are very good. Even in the case of such a large diffuse source as 0538+498 where the jet extends for ~200 mas (~70 beams) the main features of the full-track maps are reproduced. The tapered maps of 0538+498 and 1458+718 actually trace the diffuse extensions of the jets better than the full-track maps, mainly due to data from many short baselines in 1990 September. Long-track maps of several other complex sources became available after we had completed the mapping of the CJ1 data (0404+768 and 2342+821, Dallacasa et al. 1994; 1652+398, Conway & Wrobel 1995). Again the principal features of the snapshot maps agree well with these recent maps and we can therefore be confident that our maps are good enough for the astronomical purposes outlined in § 2.

In order to acquire a semiquantitative view of our ability to detect extended, low surface-brightness components in a map which contains a bright compact component, we carried out some further imaging simulations. To simplify the process we did not include bright compact components in the test images and did not introduce telescope-dependent errors in the data. This allowed us to dispense with self-calibration when making images from the simulated data. Using the FAKE program in the Caltech VLBI software package, datasets corresponding to observations with a 12 telescope array (as in the 1990 September observations) were created for single Gaussian models having a range of flux densities and angular sizes. A map was made from each data set using the programs in the Caltech package. For the larger angular sizes (≥30 mas), tapering in the u, v plane and larger map and beam sizes were used.

A summary of our results is shown in Figure 3. For strong components (flux density ≥ 300 mJy), Gaussian components with sizes as large as 100 mas (FWHM) are easily detected. As the flux density decreases, larger sources become difficult to detect, for example a 30 mJy, 30 mas source is barely detected, and a 30 mJy, 100 mas source cannot be detected even on a heavily tapered map. These estimates of surface brightness sensitivity are likely to be conservative, since useful data were obtained from more than 12 telescopes in the other observing sessions. It is important to stress that in order to achieve the performance summarized in Figure

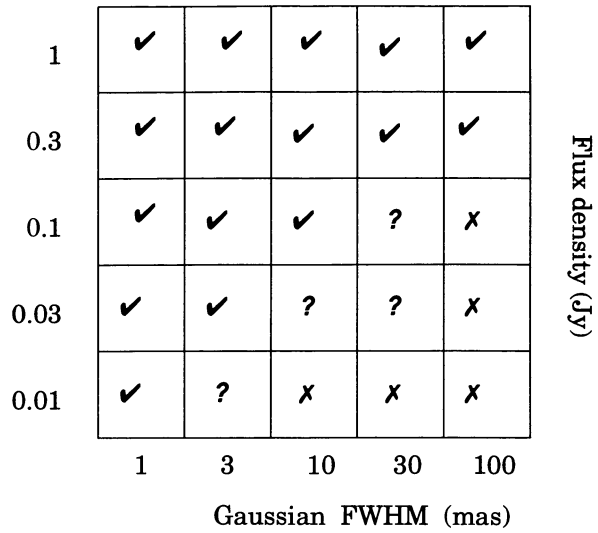

FIG. 3.—A summary of the results from the simulations to assess the sensitivity of the snapshot observing technique to weak extended components. Since in practice the data have to be self-calibrated one can achieve this performance only if the source also contains a compact component whose flux density is ~100 mJy. A tickmark in each square indicates that a Gaussian component of that size and flux density is clearly detected in the maps, a "?" that the component has probably been detected and a "χ" that there is no evidence for the component in the map.

3, with a phase-uncorrected VLBI array using Mark II equipment, the source must also contain a compact component with a flux density ~ 100 mJy. This bright component enables the data to be self-calibrated easily.

These simulations were for source components at the center of the map. Away from the source center two major effects limit the field of view: the finite bandwidth and the coherent averaging time (Thompson, Moran, & Swenson 1986). For a ~1% bandwidth and a 1 minute coherent integration time, which we used for all our data, the dominant effect is time averaging. For a reduction in amplitude of 10% the field of view for our observations is ±0.″45 from the map center.

REFERENCES

Bartel, N., Ratner, M. I., Shapiro, I. I., Cappallo, R. J., Rogers, A. E. E., & Whitney, A. R. 1985, AJ, 90, 2532
Browne, I. W. A., Patnaik, A. R., Walsh, D., & Wilkinson, P. N. 1993, MNRAS, 263, L32
Cawthorne, T. V., Wardle, J. F. C., Roberts, D. H., & Gabuzda, D. C. 1993a, ApJ, 416, 519
Cawthorne, T. V., Wardle, J. F. C., Roberts, D. H., Gabuzda, D. G., & Brown, L. F. 1993b, ApJ, 416, 496
Cohen, M. H., et al. 1975, ApJ, 201, 249.
Conway, J. E., Myers, S. T., Pearson, T. J., Readhead, A. C. S., Unwin, S. C., & Xu, W. 1994, ApJ, 425, 568
Conway, J. E., & Wrobel, J. M. 1995, ApJ, 439, 98
Dallacasa, D., Fanti, C., Fanti, R., Schilizzi, R. T., Spencer, R. E., & Venturi, T. 1990, in Compact Steep-Spectrum and GHz-peaked Spectrum Radio Sources, ed. C. Fanti, R. Fanti, C. P. O'Dea, & R. T. Schilizzi (Bologna: Consiglio Nazionale delle Ricerche), 77
Dallacasa, D., Fanti, C., Fanti, R., Schilizzi, R. T., & Spencer, R. E. 1994, A&A, in press
Eckart, A., Witzel, A., Biermann, P., Johnston, K. J., Simon, R. S., Schalinski, C., & Kühr, H. 1987, A&AS, 67, 121
Fanti, C., Fanti, R., Parma, P., Schilizzi, R. T., & van Breugel, W. J. M. 1985, A&A, 143, 292
Fanti, R., Fanti, C., Schilizzi, R. T., Rendong, N., Parma, P., van Breugel, W. J. M., & Venturi, T. 1990a, A&A, 231, 333
Fanti, R., Fanti, C., Stanghellini, C., Schilizzi, R. T., Spencer, R. E., & van Breugel, W. J. M. 1990b, in Compact Steep-Spectrum and GHz-Peaked Spectrum Radio Sources, ed. C. Fanti, R. Fanti, C. P. O'Dea, & R. T. Schilizzi (Bologna: Consiglio Nazionale delle Ricerche), 48
Foulsham, P. A. 1989, M.Sc. thesis, Univ. of Manchester
Giovannini, G., Comoretto, G., Feretti, L., Marcaide, J., Venturi, T., Vermeulen, R., & Wehrle, A. E. 1992, in Physics of Active Galactic Nuclei, ed. W. J. Duschl & S. J. Wagner (Berlin: Springer), 561
Gurvits, L. I. 1993, in Subarcsecond Radio Astronomy, ed. R. J. Davis & R. S. Booth (Cambridge: Cambridge Univ. Press), 380
Henstock, D. R., Browne, I. W. A., Wilkinson, P. N., Taylor, G. B., Vermeulen, R. C., Pearson, T. J., & Readhead, A. C. S. 1995, ApJS, submitted
Hewitt, A., & Burbidge, G. 1993, ApJS, 87, 451
Hooimeyer, J. R. A., Barthel, P. D., Schilizzi, R. T., & Miley, G. K. 1992, A&A, 261, 61
Hough, D. H., Vermeulen, R. C., & Readhead, A. C. S. 1993, in Subarcsecond Radio Astronomy, ed. R. J. Davis & R. S. Booth (Cambridge: Cambridge Univ. Press), 193
Jackson, N. J. 1989, Ph.D. thesis, Univ. of Manchester
Jones, D. L., et al. 1986, ApJ, 305, 684
Kellermann, K. I. 1993, Nature, 361, 134
Kühr, H., Nauber, U., Pauliny-Toth, I. I. K., & Witzel, A. 1979, A catalog of radio sources, MPIfR preprint 55
Kühr, H., Pauliny-Toth, I. I. K., Witzel, A., & Schmidt, J. 1981, AJ, 86, 854 (S5)
Lawrence, C. R., Zucker, J. R., Readhead, A. C. S., Unwin, S. C., Pearson, T. J., & Xu, W. 1995, ApJS, submitted
Lind, K. R. 1987, in Superluminal Radio Sources, ed. J. A. Zensus & T. J. Pearson (Cambridge: Cambridge Univ. Press), 180
Napier, P. J., Bagri, D. S., Clark, B. G., Rogers, A. E. E., Romney, J. D., Thompson, A. R., & Walker, R. C. 1994, Proc. IEEE, 82, 658
Owen, F. N., Wills, B. J., & Wills, D. 1980, ApJ, 235, L57
Patnaik, A. R., Browne, I. W. A., Wilkinson, P. N., & Wrobel, J. M. 1992, MNRAS, 254, 655
Pauliny-Toth, I. I. K., Witzel, A., Preuss, E., Kühr, H., Kellermann, K. I., Fomalont, E. B., & Davis, M. M. 1978, AJ, 83, 451 (S4)
Peacock, J. A., & Wall, J. V. 1982, MNRAS, 198, 843
Pearson, T. J. 1991, BAAS, 23, 991
Pearson, T. J., & Readhead, A. C. S. 1981, ApJ, 248, 61

Pearson, T. J., & Readhead, A. C. S. 1984, ARA&A, 22, 97
———. 1988, ApJ, 328, 114 (PR88)
Polatidis, A. G. 1993, Ph.D. thesis, Univ. of Manchester
Preston, R. A., Morabito, D. D., Williams, J. G., Faulkner, J., Jauncey, D., & Nicholson, G. D. 1985, AJ, 90, 1599
Readhead, A. C. S., Pearson, T. J., & Unwin, S. C. 1984, in IAU Symp. 110, VLBI and Compact Radio Sources, ed. R. Fanti, K. I. Kellermann, & G. Setti (Dordrecht: Reidel), 131
Sanghera, H. S. 1989, M.Sc. thesis, Univ. of Manchester
———. 1992, Ph.D. thesis, Univ. of Manchester
Schwab, F. R., & Cotton, W. D. 1983, AJ, 88, 688
Shepherd, M. C., Pearson, T. J., & Taylor, G. B. 1994, BAAS, 26, 987
Simon, R. S., Readhead, A. C. S., & Wilkinson, P. N. 1984, in IAU Symp. 110, VLBI and Compact Radio Sources, ed. R. Fanti, K. I. Kellermann, & G. Setti (Dordrecht: Reidel), 111
Spinrad, H., Djorgovski, S., Marr, J., & Aguilar, L. 1985, PASP, 97, 932
Stickel, M., & Kühr, H. 1994, A&AS, 103, 349
Stickel, M., Meisenheimer, K., & Kühr, H. 1994, A&AS, 105, 211
Taylor, G. B., Vermeulen, R. C., Pearson, T. J., Readhead, A. C. S., Henstock, D. R., Browne, I. W. A., & Wilkinson, P. N. 1994, ApJS, 95, 345
Thakkar, D. D., Pearson, T. J., Readhead, A. C. S., Xu, W., Taylor, G. B., Vermeulen, R. C., Polatidis, A. G., & Wilkinson, P. N. 1995, ApJS, 98, 33
Thompson, A. R., Moran, J. M., & Swenson, G. W. 1986, Interferometry and Synthesis in Radio Astronomy (New York: Wiley)
Vermeulen, R. C., & Cohen, M. H. 1994, ApJ, 430, 467
Wehrle, A. E., Cohen, M. H., Unwin, S. C., Aller, H. D., Aller, M. F., & Nicolson, G. 1992, ApJ, 391, 589
Wilkinson, P. N. 1989, in Very Long Baseline Interferometry Techniques and Applications, ed. M. Felli & R. E. Spencer (Dordrecht: Kluwer), 69
Wilkinson, P. N., Spencer, R. E., Readhead, A. C. S., Pearson, T. J., & Simon, R. S. 1984, in IAU Symp. 110, VLBI and Compact Radio Sources, ed. R. Fanti, K. I. Kellermann, & G. Setti (Dordrecht: Reidel), 25
Wilkinson, P. N., Polatidis, A. G., Readhead, A. C. S., Xu, W., & Pearson, T. J. 1994, ApJ, 432, L87
Witzel, A., Schalinski, C. J., Johnston, K. J., Biermann, P. L., Krichbaum, T. P., Hummel, C. A., & Eckart, A. 1988, A&A, 206, 245
Xu, W., Lawrence, C. R., Readhead, A. C. S., & Pearson, T. J. 1994, AJ, 108, 395
Xu, W., Readhead, A. C. S., Pearson, T. J., Polatidis, A. G., & Wilkinson, P. N. 1995, ApJS, submitted
Zensus, J. A., & Porcas, R. W. 1987, in Superluminal Radio Sources, ed. J. A. Zensus & T. J. Pearson (Cambridge: Cambridge Univ. Press), 126